Bond Energies and Bonding Interactions in $Fe(CO)_{5-n}(N_2)_n$ ($n = 0-5$) and $Cr(CO)_{6-n}(N_2)_n$ ($n = 0-6$) Complexes: Density Functional Theory Calculations and Comparisons to Experimental Data

David L. Cedeño and Eric Weitz*

Department of Chemistry, Northwestern University, Evanston, Illinois 60208-3113

Attila Bérces†

Steacie Institute for Molecular Sciences, National Research Council of Canada, Ottawa, Ontario K1A 0R6, Canada

Received: August 29, 2000; In Final Form: February 6, 2001

Metal−N_2 bond energies have been calculated for the $Fe(CO)_{5-n}(N_2)_n$ ($n = 1-5$) and $Cr(CO)_{6-n}(N_2)_n$ ($n = 1-6$) complexes using density-functional theory (DFT). Bond enthalpies calculated using the gradient corrected BP86 functional are in good agreement with the available experimental data. An energy decomposition procedure and a population analysis were performed for all of the complexes to quantitatively characterize the interactions of N_2 and CO with the relevant coordinatively unsaturated metal species. In all cases, the metal−N_2 bond is weaker than the metal−CO bond because CO is both a better donor and a better acceptor of electron density. Calculated bond energies for Cr−N_2 bonds for the lowest energy isomers of the chromium complexes are 24, 23, 22, 21, 20, and 25 kcal/mol for $n = 1-6$, respectively. The trend of decreasing bond energy with added N_2 ligands is a result of weaker orbital interactions. The exception is $Cr(N_2)_6$, which is predicted to be more stable than the CO containing complexes. This increase in stability is ascribed to the absence of a CO trans effect. In contrast, the Fe−N_2 bond energies for the lowest energy isomers in the series are 24, 17, 14, 10, and 5 kcal/mol for $n = 1-5$, respectively. Although iron has a larger orbital interaction with dinitrogen ligands than chromium, the 16-electron iron complexes have to deform substantially when going from their ground triplet states to their final pentacoordinated singlet geometries. An energy cost that increases as the number of N_2 ligands increases is associated with this deformation. For chromium complexes, this deformation term does not significantly decrease the bond energy, but the magnitude of this term becomes the dominant factor in the differences in bond energies in the dinitrogenated iron complexes.

I. Introduction

An understanding of the metal−ligand bonding interactions is of critical importance in predicting the strength of chemical bonds and therefore the stability and reactivity of organometallic compounds. Though progress has been made in experimental determinations of bond dissociation enthalpies, there is still limited data in this area.[1] However, it is now possible to calculate the bond energies of a variety of organometallic systems using density-functional theory (DFT). The geometries, frequencies, and bond energies that are obtained are generally as good or better than those obtained using Hartree−Fock methods.[1−4] Furthermore, bond enthalpies calculated using DFT are generally in good agreement with experimental values, provided that an appropriate exchange-correlation functional is chosen. In addition, methods have been developed to decompose the resulting metal−ligand interaction energy into terms related to the attractive and repulsive nature of the orbital interactions.[5−7] The algebraic sum of such terms is the energy of a metal−ligand bond. Such energy decomposition methods combined with an analysis of the change in electron population of the interacting orbitals of the metal and the ligand provide useful insights into the factors that determine bond strengths.

All of the complexes in the chromium series $Cr(CO)_{6-n}(N_2)_n$ ($n = 1-6$) have been experimentally observed.[8,9] When data on lifetimes exist, the trend is that the stability of the complexes decreases in parallel with an increase in the number of dinitrogen ligands. The available data are more limited for the iron complexes $Fe(CO)_{5-n}(N_2)_n$ ($n = 1-5$), but their stability seems to follow the same qualitative trend: the monodinitrogen is more stable than the bisdinitrogen[10] and both are much more stable than the pentadinitrogen complex.[11] These trends clearly indicate that the metal−N_2 bond energy is not constant as the number of nitrogen ligands increases. Interestingly, the chromium complexes seem to be more stable than the corresponding iron species. This is at least superficially in opposition to the general view that dinitrogen forms more stable complexes with electron-rich metals.[12] This paper focuses on an analysis of the bonding interactions between dinitrogen and the metal centers in these series in order to understand the differences in stability between the corresponding chromium and iron complexes, as well as trends in the stability of complexes within a given series. Both energy decomposition and population analysis are used to quantitatively analyze the bonding in the various metal−N_2 complexes. Additionally, the effect of consecutive dinitrogen substitution on the bonding of the C−O ligands to the metal centers is analyzed and discussed. Results are compared to available experimental data with a focus on recent data from

* To whom correspondence should be addressed.
† Present Address: Novartis Forschungsinstitut Gmbh, A-1235 Vienna, Austria.

10.1021/jp003097k CCC: $20.00
Published on Web 03/27/2001

our laboratory involving measurements of the bond dissociation enthalpies of $Fe(CO)_4(N_2)$ and $Fe(CO)_3(N_2)_2$.[10]

II. Methodology

Geometries and energies were calculated with the Jaguar[13] quantum chemistry software using the pseudospectral method.[14] All calculations were performed using DFT and the local density approximation (LDA), with the exchange Xα potential by Slater[15] and the correlation method of Vosko et al. (VWN).[16] Nonlocal density functionals were added self-consistently. Becke's 88[17] was used for exchange and Perdew's 86[18] for correlation. Two different basis sets were employed: LACVP** and LACV3P**. Both use Hay and Wadt's effective core potential (ECP)[19] basis sets for Fe and Cr, in which the outermost core orbitals are included. LACV3P is a triple-ζ contraction of the LACVP.[20] For C, O, and N atoms, LACVP** uses the 6-31G** basis[21] and LACV3P** uses the 6-311G** basis.[22]

Where indicated, unscaled frequencies were calculated for optimized geometries using analytical second derivatives of the energy gradients and the same functional that was used for energy minimization. Vibrational frequencies of transition metal carbonyls can be predicted with good accuracy (2−10%) by DFT methods provided that a good initial reference geometry is available.[23,24]

The calculated bond energies (ΔE_e) are defined[1] as the difference in the total energies of the optimized products and reactants for the reaction

$$ML_n \rightarrow ML_{n-1} + L$$

$$\Delta E_e = E(ML_{n-1}) + E(L) - E(ML_n) \quad (1)$$

Thus, by this definition, *factors that increase bonding interactions are positive*. The bond enthalpy at 298 K (ΔH_{298}) is calculated[25] from ΔE_e after algebraic addition of the zero-point vibrational energy (ΔZPE), the thermal energy content (ΔE_{th}), the molar work [Δ(PV)], and the basis set superposition error (BSSE) as shown in eq 2.

$$\Delta H_{298} = \Delta E_e + \Delta ZPE + \Delta E_{th} + BSSE + \Delta(PV) \quad (2)$$

Zero-point energies used in this calculation are based on the frequency calculations. The molar work term assumes ideal gas behavior and is equal to *RT* for a ligand dissociation reaction. The thermal energy content (ΔE_{th}) is the sum of the changes in translational, rotational, and vibrational energy when going from 0 to 298 K. BSSEs were estimated by running a counterpoise calculation[26] and, in terms of the sign convention used here, are negative.

The bond energy decomposition analysis was performed using the Amsterdam density-functional program (ADF99).[27] The analysis is based on an extended transition-state method.[5,6] All energy decomposition analyses were performed using the same BP86 functional used for energy minimization. However, when using ADF, the atomic orbitals on the metals were described by an uncontracted triple-ζ STO basis set,[28] whereas a double-ζ STO basis set was used for carbon, nitrogen, and oxygen. A single-ζ polarization function was used on all atoms. The $1s^2 2s^2 2p^6$ configuration of the metals and the $1s^2$ configuration on carbon, nitrogen, and oxygen were assigned to the core and treated by the frozen core approximation.[27b] A set of auxiliary s, p, d, f, g, and h STO functions, centered on all nuclei, were used in order to fit the molecular density and represent the Coulomb and exchange potentials accurately in each SCF cycle.[29] In the energy decomposition analysis, the bond energy (ΔE_e) is the result of the contributions from three terms:

$$\Delta E_e = \Delta E_{oi} + \Delta E_{steric} + \Delta E_{def} \quad (3)$$

ΔE_{def} is the energy necessary to deform the bonding moieties from their respective isolated equilibrium geometries into the geometries they assume in the bound complex. ΔE_{steric} is the sum of two terms, one corresponding to the electrostatic interaction between the fragments and the other corresponding to the Pauli repulsion. ΔE_{oi} is the energy due to the interactions between the occupied orbitals of one fragment and the empty orbitals of the other fragment, as well as between the occupied and empty orbitals within a given fragment (polarization). ΔE_{oi} is decomposed into a sum of terms which contains a term for each irreducible representation of the interacting orbitals. Additionally, for each system, a Mulliken population analysis[30] was performed in order to evaluate the population change occurring when the ligand and metal fragments interact. When comparing one complex to another, some of the calculated energy differences are within the error limits of the level of theory used. However, we focus on *trends* in bond energies and the contributions of various factors to these bond energies. When possible the calculated results are compared to experimental data.

III. Results and Discussion

A. Calibration Systems: $Fe(CO)_5$ and $Cr(CO)_6$. Calculations were performed for $Fe(CO)_5$ and $Cr(CO)_6$ using both the LACVP** and the LACV3P** basis sets. The results were compared with available experimental data as well as previously calculated geometries and bond enthalpies. Table 1 is a summary of the optimized geometries resulting from these calculations, available experimental data,[31−33] and some prior theoretical results.[23,34−36] In general, there is a very good agreement between the experimental and calculated geometrical data. However, most DFT calculations give an axial Fe−C bond that is slightly longer than the equatorial Fe−C bond, whereas the experimental data disagrees on this question. The main differences between the results obtained using the LACVP** and LACV3P** basis sets is that C−O and N−N bond lengths are ∼0.01 Å longer and the metal−ligand distances are ∼0.01 Å shorter when LACVP** is used. However, the larger basis set gives metal−ligand and C−O bond lengths closer to experimental values. Table 2 contains calculated bond energies and bond enthalpies, as well as relevant experimental data[38,39] along with some other theoretical results.[34−36,40−44] Both basis sets yield similar values for ΔE_e. However, values obtained with the smaller basis set are larger by ∼1−2 kcal/mol. These differences could simply be due to differences in the BSSE, which is ∼2−3 kcal/mol for the smaller basis set and 1−2 kcal/mol for the larger one. In general, there is good agreement between the various DFT/BP86 methods (see Table 1). Interestingly, all of the BP86 calculations reproduce the experimental bond enthalpies better than those obtained using the BLYP or B3LYP functionals (see the Supporting Material). These latter functionals were found to underestimate the bond energies.[35] As a calibration, the $Fe(CO)_5$ bond energies were calculated relative to the C_{2v} triplet state of $Fe(CO)_4$, which is the experimentally determined ground state.[45] $Cr(CO)_6$ bond energies are relative to the C_{4v} singlet ground state of $Cr(CO)_5$.[46] Geometrical parameters calculated for both unsaturated species can be found in the Supporting Material.

After it was demonstrated that the calculations agreed with the experiment for $Fe(CO)_5$ and $Cr(CO)_6$ using the BP86

TABLE 1: Calculated and Experimental Geometrical Parameters[a] for $Fe(CO)_5$, $Cr(CO)_6$, CO and N_2

	BP86−I[b]	BP86−II[b]	BP86−WW[c]	BP86−BZ[d]	BP86-vW[e]	Exp[f]	Exp[g]
$Fe(CO)_5$	D_{3h}						
$Fe-C_{ax}$	1.794	1.804	1.810	1.819	1.802	1.807	1.811
$Fe-C_{eq}$	1.792	1.800	1.807	1.817	1.797	1.827	1.803
$C-O_{ax}$	1.160	1.152	1.162	1.152	1.158	1.152	1.117
$C-O_{eq}$	1.163	1.155	1.165	1.156	1.161	1.152	1.133

	BP86−I[b]	BP86−II[b]	BP86−BZ[d]	BP86-vW[e]	BP86−B[h]	Exp[i]	Exp[i]
$Cr(CO)_6$	O_h						
Cr−C	1.894	1.907	1.917	1.909	1.929	1.916	1.918
C−O	1.162	1.153	1.154	1.159	1.155	1.147	1.141

	BP86−I[b]	BP86−II[b]	BP86-vW[e]	BP86−B[h]	Exp[e]	Exp[j]
Free CO	1.148	1.138	1.145	1.137	1.128	1.115

	BP86−I[b]	BP86−II[b]	BP86-vW[e]	Exp[e]
Free N_2	1.116	1.106	1.113	1.098

[a] Although data has been previously reported for other DFT functionals, only BP86 data, which is relevant to the method calibration, are presented in this table. Bond lengths in angstroms, angles in degrees. [b] This work, I = LACVP** basis set; II = LACV3P** basis set. [c] Reference 35. [d] Reference 23. [e] Reference 34. [f] Reference 31. [g] Reference 32. [h] Reference 36. [i] Reference 33. [j] Reference 37.

TABLE 2: Calculated and Experimental Bond Energies and Enthalpies[a] for CO Dissociation from $Fe(CO)_5$ and $Cr(CO)_6$

$Fe(CO)_5$			$Cr(CO)_6$		
	ΔE_e	ΔH_{298}		ΔE_e	ΔH_{298}
BP86-I[b]	48.9	43.9	BP86-I[b]	45.4	41.7
BP86-II[b]	46.8	43.4	BP86-II[b]	44.0	41.2
BP86-WW[c]	45.4	44.9	BP86-B[j]	40.8	
BP86-LSZ[d]	44.8		BP86-vW[e]	42.6	
BP86-vW[e]	45.9		CCSD(T)/MP2[k]	45.8	
BP86-H[f]		42.3	experiment[i]		37 ± 2
BLYP-WW[c]	37.9	37.5	experiment[l]		37 ± 5
BLYP-DWL[g]	41				
B3LYP-WW[c]	30.0	29.7			
CCSD(T)/MP2[h]	46.9				
experiment[i]		41 ± 2			

[a] Energies in kcal/mol. [b] This work, I = LACVP** basis set, II = LACV3P** basis set. [c] Reference 35. [d] Reference 40. [e] Reference 34. [f] Reference 41. [g] Reference 42. [h] Reference 43. [i] Gas-phase laser pyrolysis from ref 38. [j] Reference 36. [k] Reference 51. [l] Heptane solution from ref 39.

TABLE 3: Calculated and Experimental Frequencies and Bond Energies and Enthalpies[a] for $Fe(CO)_4(N_2)$

	frequencies[b]			
	equatorial N_2		axial N_2	
	BP86−I[c]	experiment[d]		BP86−I[c]
ν_{N-N}	2217 (0.05)	2235 (0.07)	ν_{N-N}	2136 (0.11)
ν_{C-O}	2022 (0.13)	2083 (0.21)	ν_{C-O}	2041 (0.11)
	1989 (1.00)	1972 (1.00)		1977 (0.54)
	1974 (0.79)	2006 (0.88)		1975 (1.00)
	1966 (0.15)	1982 (0.48)		

	ΔE_e	ΔH_{298}		ΔE_e	ΔH_{298}
BP86-I[c]	23.5	19.8	BP86-I	22.9	18.6
BP86-II[c]	22.7	19.0			
experiment[e]		17.6 ± 1.8			

[a] Energies in kcal/mol. [b] Frequencies in cm^{-1}; relative intensities in parentheses. [c] Basis set I = LACVP**; set II = LACV3P**. [d] Polyethylene matrix from ref 48b. [e] Gas phase from ref 10.

functional and the chosen basis sets, geometries, bond energies, and frequencies were calculated for the dinitrogen substituted complexes. Although there are examples in which N_2 is bound to a metal center in an η^2 (side-on) fashion,[47] it is well established[12,47] that the typical coordination for N_2 is in a η_1 (end-on) fashion. Consistent with this expectations, a calculation for η^1 and η^2 isomers of $Fe(CO)_4N_2$ revealed that the η^1 isomer is more stable than the η^2 isomer by 13 kcal/mol. This is in agreement with previous calculations by Hoffmann and co-workers.[41] Therefore only η^1-bound N_2 complexes are considered in this paper. To make the most effective use of computational time, all of the calculations were performed with the LACVP** basis. Additional calculations, using the LACV3P** basis set, were also performed for complexes that have experimentally known metal−ligand bond enthalpies: $Fe(CO)_4(N_2)$, $Fe(CO)_3(N_2)_2$, and $Cr(CO)_5(N_2)$.

An issue arising from the fact that $Fe(CO)_4$ has a triplet ground state is whether the unsaturated 16-electron $Fe(CO)_{4-n}(N_2)_n$ ($n = 1-4$) species have triplet or singlet ground states. Our calculations with the LACVP** basis set indicate that all of the triplet states are lower in energy than the singlet states. Past DFT calculations[35,48] on systems (FeCO and $Fe(CO)_4^+$) for which there are known experimental data suggest that, contrary to what is found for Hartree−Fock methods, there is no significant energy bias toward the higher multiplicity state. Our own calculation on FeCO supports this argument. In general, the triplet−singlet energy differences are in the 1−6 kcal/mol range, increasing with the number of N_2 ligands (see the Supporting Material). However, for some of these systems, especially where there is no relevant experimental data, the energy differences between the lowest energy state and the next highest state, which is a singlet, may be too close to definitively state that these complexes have triplet ground states.

B. Iron Carbonyl−Dinitrogen Complexes: Comparison to Experiment. $Fe(CO)_4(N_2)$ has been observed in both matrices[49] and in the gas phase.[10,50] On the basis of the number and positions of the observed infrared absorptions, Cooper and Poliakoff[49b] assigned a C_{2v} geometry to the complex. In this complex, N_2 occupies an equatorial position. Table 3 shows the calculated results for both the axial (C_{3v}) and equatorial (C_{2v}) $Fe(CO)_4N_2$ complexes. Our calculations agree that the equatorial isomer is more stable than the axial isomer, although not by much (0.6 kcal/mol). However, the frequencies reported here and those by Hoffmann and co-workers[41] clearly corroborate the assignment made by Poliakoff for the equatorial isomer.

TABLE 4: Calculated and Experimental Bond Energies and Enthalpies[a] for $Fe(CO)_3(N_2)_2$

$Fe(CO)_3(N_2)_2$	cis-(e,a)	cis-(e,e)	trans-(a,a)
ΔE_e	17.3	15.2	12.5
ΔH_{298}	13.6	11.4	8.1
ΔH (exp)[b]	9.0 ± 4.6		

[a] Energies in kcal/mol. [b] Gas phase from ref 10.

The calculated values of 19.8 and 19.0 kcal/mol for the $Fe-N_2$ bond enthalpy agrees very well with the experimental value of 17.6 ± 1.8 kcal/mol determined by Wang et al.[10] in the gas phase. It also agrees very well with the value of 19.0 kcal/mol calculated by Hoffmann and co-workers[41] using DFT with a Slater orbitals basis set and the BP86 functional. The absence of experimental evidence for a second isomer in both the ambient-temperature gas-phase work and in the low-temperature studies implies that either the two isomers are not in equilibrium or that there is a larger energy difference between the axial (C_{3v}) and equatorial (C_{2v}) isomer than the calculated value of 0.6 kcal/mol. In any case, the agreement between experimental and calculated frequencies makes a compelling case that the equatorial isomer (C_{2v}) is the lowest energy form of $Fe(CO)_4N_2$.

The bisdinitrogen species, $Fe(CO)_3(N_2)_2$, has recently been detected in the gas phase by Wang et al.[10] Three different isomers of $Fe(CO)_3(N_2)_2$ are possible: one in which both N_2 ligands are in the axial position (trans isomer), one in which both are in the equatorial position (cis-(e,e) isomer), and one in which one N_2 is axial and the other is equatorial (cis-(a,e) isomer).

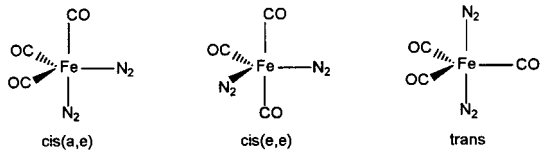

The calculations presented in Table 4 indicate that the cis-(a,e) isomer is the most stable, followed by the cis-(e,e) (higher by 2.1 kcal/mol), and finally the trans isomer (higher by 4.8 kcal/mol). The bond energies were calculated relative to the lowest energy triplet state of $Fe(CO)_3(N_2)$. The ground-state triplet has the N_2 ligand in a pseudoaxial position, suggesting that dissociation of the equatorial N_2 is the lowest energy pathway. There is a singlet state of $Fe(CO)_3(N_2)$ and another triplet state (N_2 is pseudoequatorial) that are calculated to be 0.9 and 4.1 kcal/mol, respectively, above the triplet ground state. On the basis of the energy differences, only the lowest energy triplet and singlet states are considered for assignment of the experimental observations. There is clearly much agreement (see Figure 1a) between the infrared absorptions that have been observed for $Fe(CO)_3(N_2)$ in the gas phase and the frequencies and intensities calculated for the lower energy triplet (relative error <1% for two absorptions). Although the energy differences in themselves would not lead to a compelling assignment of the ground state of $Fe(CO)_3(N_2)$ as a triplet, the positions of the lowest energy singlet absorptions and their intensities are significantly different (relative errors are >1% and 2%) than what is observed. As such, we assign the ground state of $Fe(CO)_3(N_2)$ as a triplet. The assignment is consistent with the slow addition of N_2 to $Fe(CO)_3(N_2)$, which would be expected for an association reaction involving a change in spin.[10]

For $Fe(CO)_3(N_2)_2$, the calculated bond energies are again not sufficiently different to provide clear evidence as to which isomer is the most stable. Wang et al. report a value of 9.0 ± 4.6 kcal/mol for the $Fe-N_2$ bond enthalpy, whereas the calculated values are 13.6, 11.4, and 8.1 kcal/mol for the cis-(a,e), cis-(e,e), and trans isomers, respectively. Three absorption bands were experimentally detected in the CO stretch region which have been assigned to $Fe(CO)_3(N_2)_2$.[10] The trans isomer is only expected to have one absorption in the CO stretching region, and therefore, it is excluded. Calculations indicate that the other two isomers should have their most intense band at the same frequency (see Figure 1b). However, the cis-(e−e) should have a medium-intensity band ~20 cm^{-1} below the more intense band, and the cis-(a,e) isomer should have a band of medium intensity ~20 cm^{-1} above the more intense band. An absorption has been detected at ~2026 cm^{-1}, but its intensity relative to the absorption at 1992 cm^{-1} could not be definitively established.[10] The absence of an experimental determination of the relative intensity of these two absorptions along with the similarity in calculated energies effectively precludes a definitive assignment as to which of the two isomers is the lower energy species. However, we tentatively assign the observed absorptions to the cis-(a,e) isomer based on two factors. One is the error in the calculated frequencies relative to the experimental frequencies. Errors of 2.8% and 2.0% are found for the cis-(e,e) isomer, whereas the they are 1.7% and 1.1% for the cis-(a,e) isomer. A second factor is that calculations predict a medium-intensity band almost overlapping the high-intensity band for the cis-(a,e) isomer. The spectral resolution in the experiments by Wang et al. is not enough to resolve these bands, but the 1992 cm^{-1} band has some asymmetry on the low frequency side that suggests the presence of a less intense, low energy shoulder. It should be noted that the isomer calculated to be the lowest in energy (cis-(a,e)) also has a greater similarity between observed and calculated absorptions and thus is tentatively assigned as the lowest energy $Fe(CO)_3(N_2)_2$ isomer (Figure 1b).

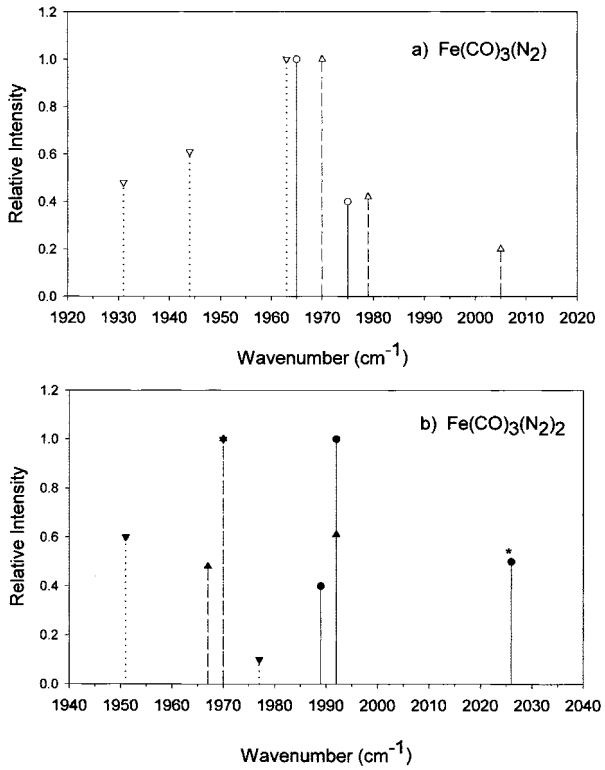

Figure 1. (a) Calculated and experimental C−O stretching frequencies for $Fe(CO)_3(N_2)$: (○—) experimental, (△- - -) calculated for triplet, (▽···) calculated for singlet. (b) Calculated and experimental C−O stretching frequencies for $Fe(CO)_3(N_2)_2$: (●—) experimental, (▲- - -) calculated for cis-(a,e) isomer, (▼···) calculated for cis-(e,e) isomer. Asterisk denotes undetermined experimental intensity.

TABLE 5: Calculated Frequencies and Bond Energies and Enthalpies[a] for cis-(a,e) $Fe(CO)_2(N_2)_3$, Equatorial-$Fe(CO)(N_2)_4$, and $Fe(N_2)_5$

	$Fe(CO)_2(N_2)_3$	$Fe(CO)(N_2)_4$	$Fe(N_2)_5$	
frequencies[b]		calculated		expt[c]
ν_{N-N}	2115 (0.17)	2292 (1.00)	2082 (1.00)	2012 (1.0)
	2068 (0.54)	2122 (0.72)	2059 (0.77)	2106 (0.6)
	2067 (1.00)	2082 (0.86)		
		2065 (0.48)		
ν_{C-O}	1999 (0.94)	2054		
	1967 (1.00)			
ΔE_e	13.8	9.6	5.1	
ΔH_{298}	9	5	1	

[a] Energies in kcal/mol. [b] Frequencies in cm^{-1}; relative intensities in parentheses. [c] 100% N_2 matrix from ref 11.

To our knowledge, $Fe(CO)_2(N_2)_3$ and $Fe(CO)(N_2)_4$ have not been experimentally observed, probably because they are both difficult to form in matrices and relatively unstable. $Fe(CO)_2(N_2)_3$ has three possible isomers. The cis-(a,e) isomer is calculated to be the most stable. It is located 2.5 and 6.5 kcal/mol below the cis-(e,e) and the trans isomers, respectively. The tetradinitrogen complex has two isomers. The isomer with an equatorial CO is calculated to be 1.8 kcal/mol more stable than the axial CO isomer. As with the other dinitrogen species, the calculated bond energies are relative to the lower energy triplet state of the unsaturated species and are shown in Table 5. The trisdinitrogen species is calculated to be more stable than the tetradinitrogen: The weakest $Fe-N_2$ bond in $Fe(CO)_2(N_2)_3$ and $Fe(CO)(N_2)_4$ including thermal and BSSE corrections has enthalpies of approximately 9 and 5 kcal/mol, respectively.

$Fe(N_2)_5$ has been previously observed in a >50% nitrogen matrix at 15 K,[11] but it readily decomposes at 40 K. $Fe(N_2)_5$ is geometrically similar to $Fe(CO)_5$, taking into account the expected differences in Fe−N and Fe−C bond lengths. $Fe(N_2)_4$ with C_{2v} symmetry is calculated to have a triplet ground state that is located 6.3 kcal/mol below the lowest energy singlet state. A bond energy of 5.1 kcal/mol is calculated relative to this triplet state. Considering the corrections to the energy, the standard bond enthalpy is ~1 kcal/mol, indicating that the $Fe(N_2)_5$ is very unstable, consistent with the report of its decomposition at temperatures above 40 K. There is also fairly good agreement (<4%) between the experimentally determined and the calculated frequencies (see Table 5).

C. Chromium Carbonyl-Dinitrogen Complexes: Comparison to Experiment. Although all of the complexes in the $Cr(CO)_{6-n}(N_2)_n$ series have been observed in matrix experiments,[8] the only bond enthalpy that has been experimentally determined is that for the $Cr-N_2$ bond in $Cr(CO)_5(N_2)$. The bond energy (ΔE_e) calculations agree well with prior DFT[34] and CCSD(T)//MP2[51] calculations. The $Cr-N_2$ bond enthalpy was calculated relative to the known singlet C_{4v} ground state[46] of $Cr(CO)_5$ (see Table 6). A value of 21.1 kcal/mol is obtained, which agrees well with the experimental value of 19 ± 1 obtained by Poliakoff and co-workers.[52]

Table 7 contains the calculated bond energies, frequencies, and intensities for all of the other chromium complexes. All bond energies are relative to the lowest energy singlet ground state of the $Cr(CO)_{6-n}(N_2)_{n-1}$ complex. The agreement between the calculated frequencies and intensities and the experimental ones is satisfactory. Interestingly, the relative deviations for C−O stretching frequencies are lower (<3%) than those for N−N stretching frequencies (up to 7%). The error in the N−N frequencies is systematic and is higher in the chromium complexes than in the iron complexes. The results of calculations of the geometries of these species are given in the Supporting Information.

TABLE 6: Calculated and Experimental Frequencies and Bond Energy and Enthalpy[a] for $Cr(CO)_5(N_2)$

frequencies[b]	BP86−I[c]	experimental[d]
ν_{N-N}	2100	2237
ν_{C-O}	2034 (0.01)	2086 (0.05)
	1960 (1.00)	1975 (1.0)
	1948 (0.43)	1965 (0.3)

	ΔE_e	ΔH_{298}
BP86-I[c]	24.2	21.1
BP86-II[c]	24.3	21.5
BP86-vW[e]	21.9	
CCSD(T)//MP2[f]	24.8	
experimental[g]		19 ± 1

[a] Energies in kcal/mol. [b] Frequencies in cm^{-1}; relative intensities in parentheses. [c] This work, I = LACVP** basis; II = LACV3P** basis. [d] Reference 8e. Includes BSSE correction from ref 34. [f] Reference 51. [g] Heptane solution from ref 52.

TABLE 7: Calculated and Experimental Frequencies and Bond Energies for $Cr(CO)_{6-n}(N_2)_n$ ($n = 2-6$)[a]

	$n = 2$ (cis isomer)		$n = 3$ (fac isomer)	
	calculated	experiment[b]	calculated	experiment[b]
ν_{N-N}	2083 (1.00)	2241 (1.0)	2207 (0.33)	2241 (0.4)
	2070 (0.21)	2220 (1.0)	2068 (1.00)	2207 (1.0)
ν_{C-O}	2036 (0.05)	2052 (0.1)	1966 (0.71)	1995 (0.7)
	1958 (1.00)	1961 (1.0)	1950 (1.0)	1932 (1.0)
	1951 (0.53)	1943 (0.5)		
	1950 (0.15)	1967 (0.2)		
ΔE_e	22.8	21[c]	21.9	19[c]

	$n = 4$ (cis isomer)		$n = 5$	
	calculated	experiment[b]	calculated	experiment[b]
ν_{N-N}	2180 (0.31)	2234 ? (w)	2210 (0.06)	2236 (0.1)
	2066 (0.37)	2194 (0.3)	2057 (1.00)	2127 (1.0)
	2059 (1.00)	2142 (1.0)		
	2045 (0.01)	2165 (v.w)		
ν_{C-O}	1950 (0.97)	1955 (1.0)	1929	1927 ?
	1936 (1.00)	1920 (1.0)		
ΔE_e	20.9		20.0	

	$n = 6$	
	calculated	experiment[d]
ν_{N-N}	2057	2120
ΔE_e	25.2	

[a] Calculated from optimized geometries using LACVP** basis set, energies in kcal/mol; frequencies in cm^{-1} and relative intensities in parentheses [b] Reference 8. [c] Values are estimated from reported lifetimes in ref 8. [d] Reference 9.

There are two $Cr(CO)_4(N_2)_2$ isomers. The calculations indicate that the cis isomer is 3.1 kcal/mol below the trans isomer. Turner et al.[8] were able to observe both isomers in a liquid xenon solution, and although they were not able to determine the relative abundance of the two isomers, they could establish that the cis isomer was more abundant. The calculated bond energy (ΔE_e) for this complex is 22.8 kcal/mol, which translates into a bond enthalpy of ~18 kcal/mol at 298 K. Although there is no report of the experimental bond enthalpy, Turner and coworkers report a half-life of ~10 min at 218 K. On the basis of this half-life, if a preexponential factor of $\sim 1 \times 10^{13}$ s^{-1} is assumed[53] for loss of N_2, an activation energy for the decay of this complex can be estimated as ~16 kcal/mol, which gives an estimated bond enthalpy of 18 kcal/mol at 298 K. This

estimate assumes that the decay of this species is due mainly to N_2 dissociation and that, as with most association reactions involving coordinatively unsaturated Cr and Fe carbonyl complexes, the reaction to form $Cr(CO)_4(N_2)_2$ from $Cr(CO)_4(N_2)$ and N_2 is unactivated. We also assume that possible complexation of solvent by the coordinatively unsaturated intermediate does not significantly effect our estimate. Given these caveats, there is good agreement between the DFT results and the estimate of the bond enthalpy that can be made from experimental observations. There is also satisfactory agreement when the calculated frequencies and intensities for $Cr(CO)_4(N_2)_2$ are compared to the experimental ones obtained by Turner and co-workers.[8]

$Cr(CO)_3(N_2)_3$ has two isomers, the fac isomer, in which all of the dinitrogens are coaxial to all of the carbonyls, and the mer isomer, which has two coaxial dinitrogen ligands.

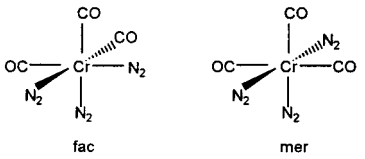

Our calculations indicate that the fac isomer is 3.1 kcal/mol lower in energy than the mer isomer. Turner et al. observed both isomers in both a CO/N_2 matrix and in liquid xenon solutions. Although the relative abundances of both isomers was not established, the intensities of the bands indicated that the fac isomer is thermodynamically preferred. They report a half-life of ~15 min at 194 K in liquid Xe, which allows a rough estimate for the bond enthalpy of the order of ~16 kcal/mol at 298 K (using the same assumptions made previously for $Cr(CO)_4(N_2)_2$). This estimate agrees reasonably well with the bond enthalpy (~17 kcal/mol) obtained from the calculated bond energy (21.9 kcal/mol).

$Cr(CO)_2(N_2)_4$ also has two isomers. The cis isomer is calculated to be 3.2 kcal/mol lower in energy than the trans isomer. In agreement with calculations, experimental data from both the liquid xenon solution and matrices suggest that the cis complex is thermodynamically more stable. Turner et al. report that $Cr(CO)_2(N_2)_4$ and $Cr(CO)(N_2)_5$ are less stable than $Cr(CO)_3(N_2)_3$ but do not report half-life data. The calculated $Cr-N_2$ bond energies (ΔE_e) are 20.9 and 20.0 kcal/mol for $Cr(CO)_2(N_2)_4$ and $Cr(CO)(N_2)_5$, respectively, continuing the experimentally observed decrease in stability trend seen for the $n = 1-3$ dinitrogen complexes.

$Cr(N_2)_6$ has been identified in a 15% Nitrogen matrix at 10 K.[9] The stability of the complex has not been experimentally quantified. The $Cr-N_2$ bond energy for this complex relative to the singlet $Cr(N_2)_5$ is calculated to be 25.2 kcal/mol, indicating that $Cr(N_2)_6$ should be approximately as stable as $Cr(CO)_5(N_2)_2$.

D. Description of the Metal−Ligand Bonding Interactions. From experimental and calculated data, it is clear that the metal−N_2 bond energy (and enthalpy) decreases as the number of nitrogen increases, with the exception of the $n = 6$ chromium complex. More interestingly, the $Fe-N_2$ bond energy *decreases significantly* when the number of N_2 ligands around the metal increases. In contrast, the bond energies in the series of chromium complexes *decrease only slightly* from $n = 1$ to 5 but then increase for the hexadinitrogen complex. This implies that the chromium complexes considered here have stronger metal bonds than their corresponding analogous dinitrogen iron complexes. Before going into the details of the analysis of the bond energy in terms of its decomposition from eq 3, it is useful to describe the molecular orbitals involved in the bonding interactions and how their energies change as a function of the number of dinitrogen ligands.

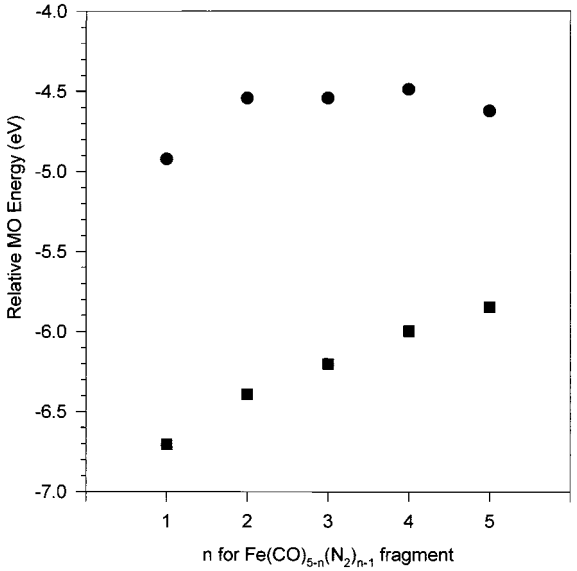

Figure 2. Energy for the HOMO (■) and LUMO (●) for $Fe(CO)_{5-n}(N_2)_{n-1}$ ($n = 1-5$) as a function of the number of N_2 ligands.

CO and N_2 are isoelectronic molecules with a lone electron pair available for bonding to the metal. In CO, the lone pair is located in the 3σ MO, whereas in N_2, it is located in the $2\sigma_g$ MO. Both of these orbitals are the HOMOs of the diatomics. The 3σ MO of CO is 1.0 eV higher in energy than the $2\sigma_g$ MO of N_2. The HOMO in N_2 is symmetrically distributed on both atoms. However, for CO, the difference in electronegativity of C versus O results in the MO being largely localized on the carbon atom. The degenerate LUMOs are the 2π MOs in CO and the π_g MOs in N_2, which are located at a similar energy.

Scheme 1 is a diagram of the frontier molecular orbitals (FMOs) showing the interaction of an $Fe(CO)_4$ fragment with an equatorial CO and an equatorial N_2. For simplicity, other metal fragments' FMOs are not shown, but the orbitals have similar splittings, although they have different energies relative to $Fe(CO)_4$ (see Figure 2). There are two main bonding interactions. One is σ donation from the ligands σ-type HOMO (σ-donor) to the σ-acceptor metal fragment LUMO ($12a_1$), which is a σ-dsp hybrid, with a large ligand contribution. The other interaction involves back-donation from the metal fragment HOMOs ($7b_1$ and $7b_2$), which are metal centered electron pairs, to the LUMO of the ligand. With the axis of the bond that is being broken or formed defined as the *z* axis, the *x* axis is then determined by the axial COs. Then the $7b_1$ MO has mainly d_{xz} character and the $7b_2$ MO has mainly d_{yz} character. Figure 2 shows the energy of the HOMO and LUMO of all of the metal fragments. As the number of N_2 ligands increases, the energy levels of the resulting metal fragment change slightly. The LUMO energy increases ~0.4 eV from $Fe(CO)_4$ to $Fe(CO)_3(N_2)$, changes little for $n = 3$ and 4, and then decreases ~0.2 eV in going from $n = 4$ to 5. An increase in the metal-fragment LUMO energy is equivalent to an increase in the energy gap for ligand to metal σ donation. This means that $Fe(CO)_4$ is the best σ acceptor and that $Fe(N_2)_4$ is a slightly better σ acceptor than the other dinitrogenated fragments. On the other hand, the metal-fragment HOMO energy increases with each additional N_2. The change in the metal fragment HOMO energy is equivalent to a narrowing of the energy gap for metal−ligand back-donation. This means that back-donation is relatively more favorable as the number of N_2 ligands increases. The relative

SCHEME 1

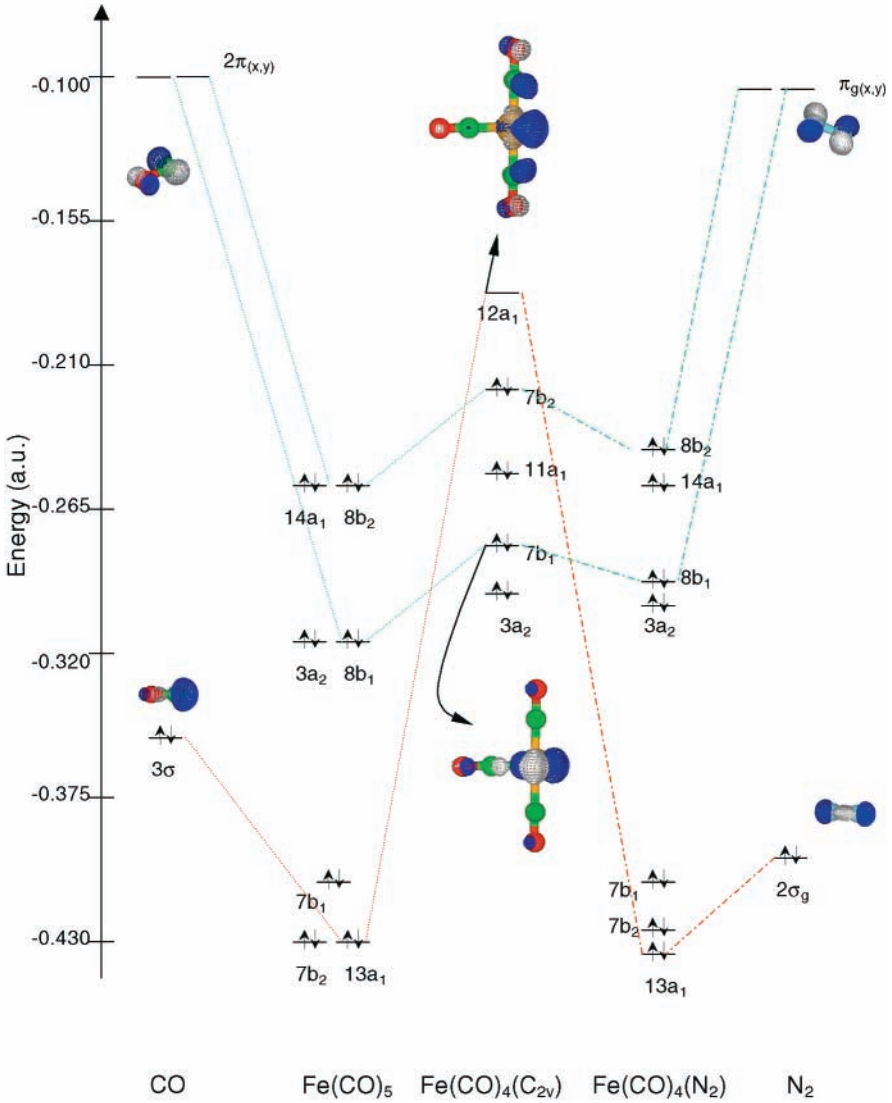

change in the $Fe-N_2$ bond energy with subsequent N_2 substitution is related to both the relative energy of the metal FMOs and their ligand overlap. Under the assumption of similar metal fragment−ligand overlap, the change in the metal FMOs energy should determine the $Fe-N_2$ interaction. For example, in going from $n = 1$ to 2, the increase in the LUMO energy is slightly larger than the increase in the HOMO energy. This implies that the increase in back-bonding capability is less than the decrease in σ accepting capability and, therefore, the $Fe-N_2$ bond energy should decrease for $n = 2$ relative to $n = 1$. When going from $n = 2$ to 3, a trend toward increasing bond energy is expected because the increment in the back-bonding capability of the fragment is larger than the change in σ-accepting character. Using the same reasoning, the $Fe-N_2$ bond energy of the $n = 4$ complex would be predicted to increase relative to the $n = 3$ species, and the bond energy for $n = 5$ would be predicted to increase relative to the bond energy of the $n = 4$ complex. These trends, which are based on the changes of energy in the HOMO and LUMO energies with increasing number of N_2 ligands, will be discussed in terms of the energy decomposition analysis in the next section.

Scheme 2 shows the frontier MO diagram for the interaction of $Cr(CO)_5$ with CO and N_2. Ligand to metal σ donation involves the $10a_1$ metal fragment MO, which is a σ-dsp hybrid with a large contribution from the ligands. This orbital accepts electron density from the σ-type MOs on both the CO and N_2 ligands. The degenerate $8e_1$ orbital (HOMO) of the chromium metal fragment is, in turn, able to donate electron density to the degenerate π LUMO of the ligand (back-donation). Figure 3 shows the HOMO and LUMO energies of the chromium fragments. The energy of the HOMO of the unsaturated chromium complexes increases with the number of N_2 ligands; the change in energy is a little larger for $n = 5$ and 6 than for $n = 1-4$. The change in the energy of the metal fragment HOMO energy leads to an increase in the back-bonding capability of the metal fragment. The LUMO energy increases with each N_2, until $n = 6$ (see Figure 3), meaning that the σ-accepting character of the metal fragment decreases slightly. *On the basis of just the relative changes of the HOMO and LUMO energies with N_2 substitution*, the $Cr-N_2$ bond energy should decrease in going from $n = 1$ to 2, $n = 2$ to 3, and $n = 3$ to 4, whereas it should increase when going from $n = 4$ to 5 and $n = 5$ to 6. A comparison of these HOMO and LUMO energy trends in the context of trends in bond energy is discussed in section III.F.

Now that the orbitals involved in bonding have been described, an analysis of the $Fe-N_2$ and $Cr-N_2$ bond energies can be performed in the context of its decomposition into deformation, attractive orbital interactions, and steric energies. Also, the change in the population of the orbitals involved as

SCHEME 2

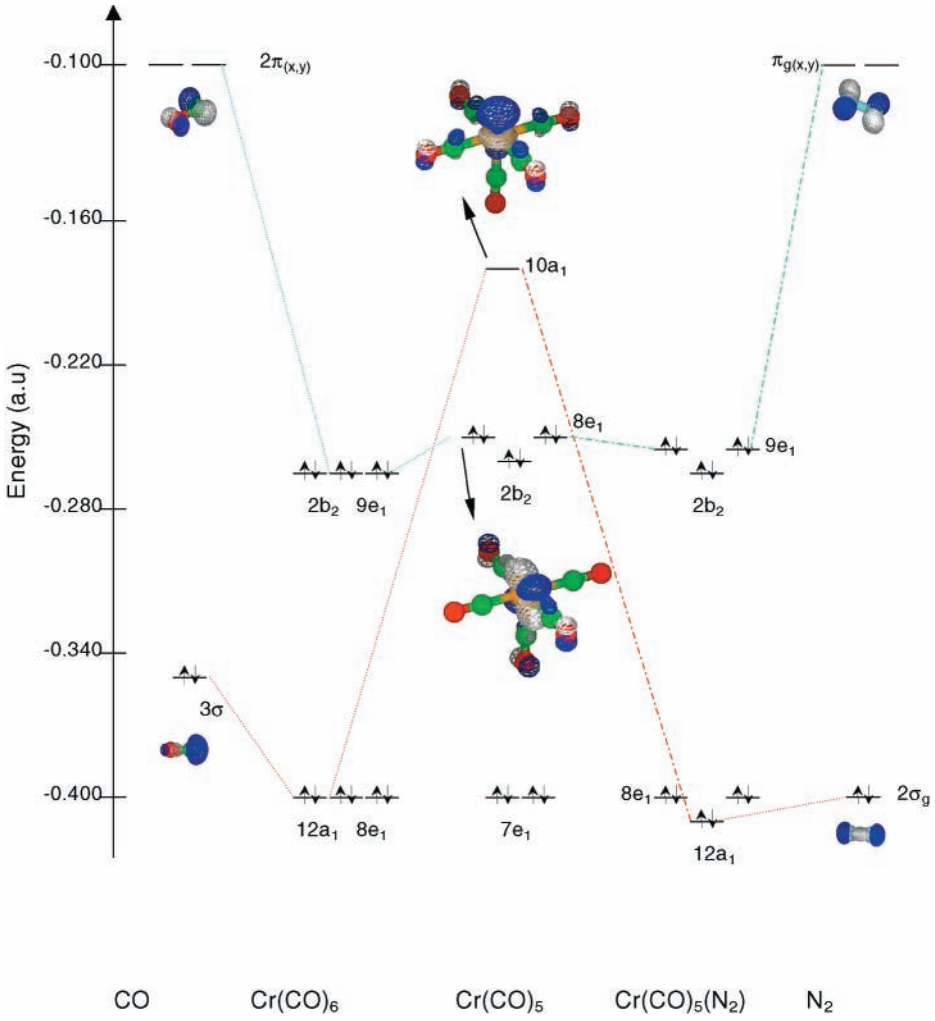

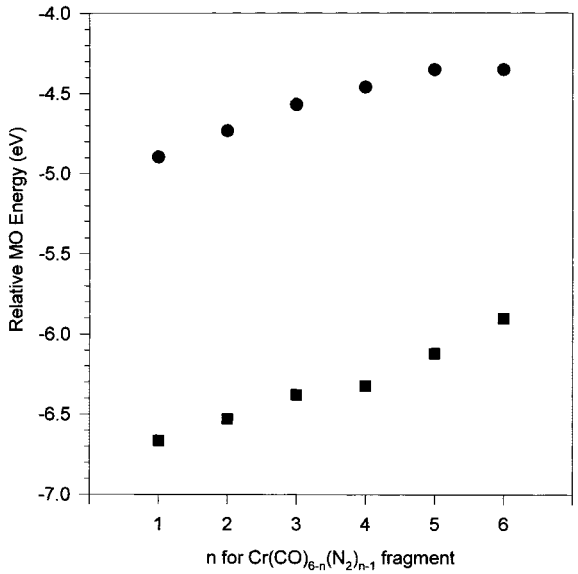

Figure 3. Energy for the HOMO (■) and LUMO (●) for $Cr(CO)_{6-n}(N_2)_{n-1}$ ($n = 1-6$) as a function of the number of N_2 ligands.

well as their overlaps will be used to understand the differences in bond energies in these two series of complexes.

E. Fe−N_2 Bond Energy in $Fe(CO)_{5-n}(N_2)_n$. Table 8 shows the changes in orbital Mulliken populations as well as the overlaps for the interacting orbitals. Figure 4 is a bar graph of

TABLE 8: Mulliken Population Change ($P(i)_j$, i = L for Ligand, or fr for Metal Fragment) and Overlap Integrals ($|\langle a_i|b_j\rangle|$) for the Interaction of Iron and Equatorial N_2 in $Fe(CO)_{5-n}(N_2)_n$

	$n=0$	$n=1$	$n=2$	$n=3$	$n=4$	$n=5$
$P(\mathrm{fr})_\sigma$	0.49	0.29	0.27	0.29	0.28	0.33
$-P(\mathrm{L})_\sigma$	0.44	0.23	0.22	0.22	0.21	0.23
$-P(\mathrm{fr})_{bb}$	0.41	0.29	0.29	0.33	0.31	0.35
$P(\mathrm{L})_{bb}$	0.44	0.30	0.29	0.32	0.31	0.35
$\lvert\langle a_1\lvert\sigma_g\rangle\rvert$	0.433	0.270	0.249	0.246	0.225	0.219
$\lvert\langle b_1\lvert\pi_x\rangle\rvert$	0.158	0.114	0.099	0.085	0.083	0.091
$\lvert\langle b_2\lvert\pi_y\rangle\rvert$	0.251	0.151	0.147	0.135	0.139	0.144

the contribution of each term in eq 3 to the total bond energy for the interaction of an equatorial ligand and the corresponding metal fragment for the lowest energy iron complexes.

The electron density lost by the HOMO σ-type orbital of the ligand is related to its donating character. In $Fe(CO)_5$, CO donates 0.44 electrons to the σ bond, whereas N_2 only donates 0.21−0.23 electrons in the dinitrogenated complexes. Similarly, the electron accepting ability of the ligand can be quantified by the gross populations of the ligand LUMO π-type orbitals. In $Fe(CO)_5$, CO accepts 0.44 electrons, whereas the population of the N_2 LUMO changes by 0.29−0.35 electrons in the dinitrogenated complexes. When compared to the change of population in the ligand HOMO, the population change in the coordinatively unsaturated metal complex LUMOs are slightly larger (0.05−0.10 electrons). An analysis of the orbital populations indicates that there is a depopulation of ∼0.08−0.11

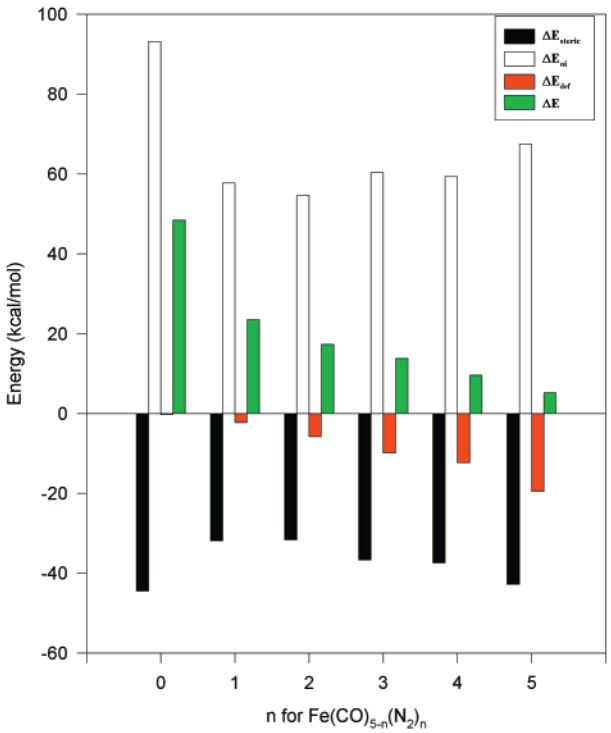

Figure 4. Energy decomposition of the interaction between an equatorial N_2 and the coordinatively unsaturated iron fragments. The decomposition for the interaction of an equatorial CO with $Fe(CO)_4$ is shown for comparison. ΔE_{steric} = steric energy; ΔE_{oi} = orbital interaction energy; ΔE_{def} = deformation energy; ΔE = bond energy.

electrons in the occupied $11a_1$ MO of the unsaturated metal carbonyl fragment. Thus, some electron density is transferred internally in the metal carbonyl (polarization) from the $11a_1$ MO to the empty LUMO ($12a_1$).

The electron donating capabilities of the ligand are also dependent on the orbital overlap. In general, CO orbitals have larger overlaps with both the donating and accepting MOs of the metal fragment than N_2 has (see Table 8). There are slight differences in the overlaps for the dinitrogenated complexes. The $2\sigma_g-12a_1$ overlap decreases as the number of N_2 ligands increases up to $n = 5$, whereas the net back-bonding overlap ($7b_1$ and $7b_2$ with $\pi_{x,y}$) decreases up to $n = 3$ and then increases. The variations in the overlap could be related to the geometrical changes taking place in the complex as the number of N_2 ligands increases. In going from the $n = 1$ to the $n = 3$ complex, the axial−axial and equatorial−equatorial angles get slightly smaller, which hinders the approach of the incoming ligand and, therefore, decreases the overlap.

The σ-donation and back-bonding capabilities of CO are superior and more balanced than those of N_2. For CO, there is a consistent balance between donating electron density and accepting it: there is a bonding synergy. For N_2, there is considerably less transfer of electron density in either direction than for CO and the back-bonding is favored. This is evident in the energy decomposition analysis: the energy contribution from both σ-donation and back-bonding for an equatorial CO in $Fe(CO)_5$ are approximately twice as large for each of these terms as they are for the $Fe-N_2$ interaction in $Fe(CO)_4(N_2)$.

The energy decomposition results in Figure 4 show that in going from $n = 1$ to $n = 2$ the orbital interaction energy (ΔE_{oi}) goes down. Replacing a CO ligand with an N_2 in the axial position is unfavorable for the bonding of an equatorial N_2 ligand. This also applies when n changes from 3 to 4. On the other hand, the energy for $n = 3$ goes up with respect to $n = 2$, which means that replacing a CO by an N_2 has a favorable effect on the electronic interaction energy. The same applies when n goes from 4 to 5. Clearly, both the energy gap between the ligand and metal MOs and their effective overlap determine the extent of the metal−ligand interaction. However, the trend in the total electronic interaction energy ($\Delta E_{oi} + \Delta E_{steric}$) as a function of the number of N_2 ligands can be qualitatively rationalized based just on the relative changes in the HOMO and LUMO of the metal, given that the changes in overlap are small. The relative changes in the total interaction energy are matched well by the relative changes in HOMO and LUMO energies, as discussed in section III.D, with the exception of the change in going from $n = 3$ to 4, which can be influenced by the slight decrease in the σ orbital overlap.

In terms of the total electronic interaction energy ($\Delta E_{oi} + \Delta E_{steric}$), the $Fe-N_2$ bond energies (ΔE_0) of the iron dinitrogen complexes should be similar (in the 22−26 kcal/mol range). However, the variation in the experimental $Fe-N_2$ bond enthalpy in going from $n = 1$ to 2 (~9 kcal/mol) indicates that just orbital interactions cannot explain the trend in the bond enthalpy. The total electronic interaction energy ($\Delta E_{oi} + \Delta E_{steric}$) would determine the bond energy if the reacting moieties would not change their geometry. However, the formation of an addition complex can require the reacting fragments to adjust their geometries to attain the equilibrium geometries they possess in the final adduct. As seen in Figure 4, for the $Fe(CO)_{5-n}(N_2)_n$ series, the magnitude of the deformation energy increases as the number of N_2 ligands increases. More importantly, this energy has a large effect on the $Fe-N_2$ bond energy of the highly dinitrogenated iron carbonyl complexes. For example, the $Fe-N_2$ total interaction ($\Delta E_{oi} + \Delta E_{steric}$) in $Fe(N_2)_5$ is 24.7 kcal/mol but the calculated bond energy is only 5.2 kcal/mol, meaning that 19.5 kcal/mol are required for the reacting moieties to rearrange to their equilibrium geometries. In terms of geometry changes, there is a 0.035 Å decrease in the $Fe-N_{eq}$ bond length in going from $^3Fe(N_2)_4$ to $Fe(N_2)_5$, whereas the $Fe-N_{ax}$ bond decreases by 0.031 Å. In addition the $N_{ax}-Fe-N_{ax}$ bond angle increases by 38°, whereas the $N_{eq}-Fe-N_{eq}$ bond angle changes by 21°. When $^3Fe(CO)_4$ adds N_2 to produce $Fe(CO)_4(N_2)$, the $Fe-C_{ax}$ bond length decreases by 0.031 Å, whereas the $Fe-C_{eq}$ bond distance only decreases 0.017 Å. Also, the $C_{eq}-Fe-C_{eq}$ bond angle increases 23°, whereas the $C_{ax}-Fe-C_{ax}$ bond angle increases by 26°. Then, the magnitudes of the deformations in $Fe(N_2)_5$ are larger than those in $Fe(CO)_4(N_2)$, consistent with a larger deformation energy for $Fe(N_2)_5$. A similar analysis done for the other 16-electron iron complexes being studied indicates that there is also a trend in the changes in geometry associated with an increase in the number of N_2 ligands. In general, the relevant bond lengths and bond angles increase gradually as the number of N_2 ligands increases.

From the analysis of the $Fe-N_2$ bond energies, it is clear that the *deformation the coordinatively unsaturated iron carbonyl moiety and the incoming ligand must undergo on bonding plays a very important role in determining the strength of the* $Fe-N_2$ *bond.* In fact, the changes in the magnitude of the $Fe-N_2$ bond energy within this series of dinitrogen complexes is dominated by changes in the magnitude of the deformation energy. The effect of deformation energy on bond dissociation energies has been recognized before both in the context of organometallic bonding[1,54,55] and in other contexts. For example, the importance of the effect of deformation energies in the calculation of bond energies by thermodynamic cycles has been previously emphasized.[1,55] Calculations performed by Weitz and co-workers[56] on iron carbonyl olefin complexes have shown

TABLE 9: Mulliken Population Changes ($P(i)_j$, i = L for Ligand, or fr for Metal Fragment) and Overlap Integrals ($|\langle a_i|b_j\rangle|$) for Cr−N_2 Interactions in $Cr(CO)_{6-n}(N_2)_n$

	$n=0$	$n=1$	$n=2$	$n=3$	$n=4^a$	$n=5^a$	$n=6$
$P(fr)_\sigma$	0.32	0.19	0.18	0.18	0.17 (0.20)	0.17 (0.19)	0.19
$-P(L)_\sigma$	0.39	0.21	0.21	0.21	0.20 (0.22)	0.20 (0.22)	0.22
$-P(fr)_{bb}$	0.34	0.24	0.24	0.24	0.25 (0.30)	0.26 (0.30)	0.30
$P(L)_{bb}$	0.40	0.26	0.27	0.27	0.27 (0.30)	0.26 (0.32)	0.32
$\|\langle a_1\|\sigma_g\rangle\|$	0.434	0.270	0.266	0.261	0.258 (0.272)	0.255 (0.270)	0.269
$\|\langle e_1\|\pi_x\rangle\|$	0.340	0.222	0.212	0.198	0.193 (0.217)	0.186 (0.210)	0.202

[a] Values in parentheses correspond to the interaction of N_2 trans to another N_2.

that the deformation of both the olefin and the coordinatively unsaturated metal fragment can significantly influence the bond energies of the olefin complexes. Such information is highly relevant to the design of catalysts for olefin isomerization. This concept also appears in other fields of chemistry.[57] In organic chemistry, strain energy is routinely taken into account when discussing bonding energetics. Another field in which the role of the deformation of the reacting moieties may play a role is enzyme catalysis. Some authors[58−60] suggest that the protein environment around the active site of enzymes adopts a conformation that is close to the unconstrained geometry of the transition state or the products. However, this issue is still under debate for enzymes because this view has been refuted by others.[61,62] Nevertheless, this concept is still not part of standard descriptions of the factors determining the bonding energetics of organometallic complexes that are found in inorganic chemistry textbooks.

It is important to recognize that for all of the iron complexes a ligand in the equatorial position *is not* equivalent to a ligand in an axial position and that the bonding of a given ligand in either position could be different. These differences can be quantified. Computations involving an energy decomposition analysis were also done for axial ligands (except for $n = 1$) and can be found in the Supporting Information. In all cases, the total interaction energies ($\Delta E_{oi} + \Delta E_{steric}$) are larger when the ligand is axial rather than equatorial. This implies that it would take more energy to break a bond to an axial ligand than a bond to an equatorial ligand, if the geometries of the reacting moieties were to remain unchanged. Also, because the final equilibrium geometry of the 16-electron species has C_{2v} symmetry, it should take less energy to deform a C_{2v} fragment produced by breaking the bond to an equatorial ligand than to deform a C_{3v} fragment obtained by breaking a bond to an axial ligand. Thus, the loss of an equatorial ligand should be favored. This picture is also consistent with the fact that the deformation energies are larger in the case of axial ligand loss.

As previously mentioned, all of the analogous chromium complexes have been experimentally detected providing even more information that can be compared to theoretical results. We now consider how the various factors that have been identified as being important in bonding in the series of dinitrogen substituted iron carbonyls effect bond strengths and trends in bonding in the analogous chromium complexes. Interestingly, we will see that the chromium complexes are more stable than the corresponding iron complexes. The factors that we explicitly consider include orbital overlaps, back-bonding, the trans effect, and the deformation energy. Once again we will see that the deformation energy plays a critical role in the fact that the dinitrogen substituted chromium complexes are more stable than their iron analogues.

F. Cr−N_2 Bond Energy in $Cr(CO)_{6-n}(N_2)_n$. Table 9 contains orbital overlaps and the change in orbital populations

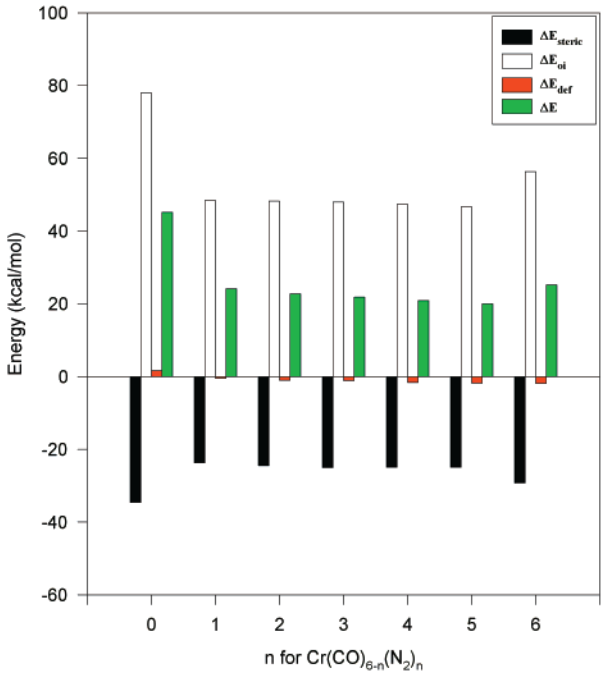

Figure 5. Energy decomposition of the interaction between N_2 and the coordinatively unsaturated chromium complexes $Cr(CO)_{5-n}(N_2)_n$ ($n = 1-5$). The decomposition of the interaction of CO with $Cr(CO)_5$ is shown for comparison. ΔE_{steric} = steric energy; ΔE_{oi} = orbital interaction energy; ΔE_{def} = deformation energy; ΔE = bond energy.

on bonding for the most thermodynamically stable chromium complexes. Figure 5 is a bar graph representation of the energy decomposition analysis for these complexes.

The change in population of the HOMO and LUMO of the ligands bound to chromium have the same trend as discussed for the iron series. The population of the $10a_1$ metal fragment LUMO is larger for $Cr(CO)_5$ than it is for dinitrogen substituted species, similar to the trend observed for the population of the $12a_1$ LUMO in the iron series. In general, the change in the population of the electron accepting ligand π orbitals and the donor metal orbitals is slightly larger (0.02−0.05 electrons) in the iron complexes than it is for the chromium complexes. Also, in the iron series, the occupied $11a_1$ is close to the LUMO ($12a_1$; see Scheme 1) and transfers electron density to the $12a_1$ MO. Such polarization is absent in the chromium complexes because it lacks a similar occupied a_1 MO (see Scheme 2). As a result of these factors the net change in the LUMO population is 0.1−0.17 more in the iron complexes than in the chromium complexes.

The orbital overlap involved in σ-donation decreases slightly from $n = 0$ to 5 for $Cr(CO)_{6-n}(N_2)_n$ but increases for $n = 6$. The overlap of orbitals involved in back-bonding exhibit the same trend. Slight variations in the geometry of the complexes could account for the variations in the extent of the orbital overlap.

As expected, CO binds more strongly than N_2: the calculated bond energy (ΔE_e) of the Cr−CO bond in $Cr(CO)_6$ is almost twice that of the Cr−N_2 bond in $Cr(CO)_5N_2$. The Cr−CO orbital interaction in $Cr(CO)_6$ is almost double that of the typical Cr−N_2 bond in the dinitrogen complexes. As with the series of iron centered complexes, the steric term has the same trend but with an opposite sign as the orbital interaction term. However, in contrast to the series of iron complexes, the trend in the total electronic interaction energy ($\Delta E_{oi} + \Delta E_{steric}$) basically parallels the trend in bond energy along the series. Thus, the main difference when comparing the metal−N_2 bond energies in the

chromium complexes relative to the corresponding iron species is that the deformation energy does not increases significantly as the number of N_2 ligands around the chromium center increases. The reaction of N_2 with $Cr(CO)_5$ leads to a 0.5 kcal/mol deformation energy, whereas reaction of $Cr(N_2)_5$ with N_2 involves a deformation energy of only 1.9 kcal/mol. In the chromium systems, the equilibrium geometries of both the isolated ligand and the isolated unsaturated species are very close to the equilibrium geometry of the final complex. The deformation in the chromium fragments involves mainly a shortening of the Cr−ligand bond trans to the vacant site ($\sim$ 0.05−0.08 Å), whereas other bonds decrease by no more than 0.02 Å, and bond angles do not change by more than 6°. These are relatively small changes when compared to the iron complexes. Thus, even though *the total orbital interaction is larger for iron, the relatively large deformation energy for the iron complexes leads to bond energies that are smaller (for n >1) than the chromium analogues with the same number of dinitrogen ligands*.

Some interesting differences are found when comparing the $Cr-N_2$ interaction for non-equivalent N_2 ligands in the same complex. The entries in parentheses for $n = 4$ and 5 in Table 11 are for the interaction of a N_2 ligand trans to another N_2 rather than trans to CO. It is clear that the net electronic interaction energy ($\Delta E_{oi} + \Delta E_{steric}$) is $\sim$5−6 kcal/mol larger for an N_2 trans to another N_2 than for an N_2 trans to a CO. This "trans effect"[12] is a manifestation of the strong back-bonding interaction between the metal and CO. The trans effect is readily apparent in the orbital interaction energy term: it is $\sim$10 kcal/mol larger in the absence of an axial CO. Though the steric term is also larger, it only changes by $\sim$5 kcal/mol. The origin of the trans effect can be studied by fragment interactions. The metal ligand interactions can change for three fundamental reasons: (1) the metal based orbitals change in energy upon trans substitution, (2) the metal based orbitals moves toward or away from the interacting ligand making the overlap differ, or (3) electrostatic interactions. In the case of N_2 and CO substitution, 1 and 2 are expected to play a major role. The changes in the energy levels of the metal fragment MOs although small ($\sim$0.2 eV) are consistent with the improved bonding interactions when there is an N_2 trans to the interacting ligand. The energy gaps between the interacting metal fragment MOs and ligand MOs are smaller when there is an N_2 ligand trans to the interacting N_2 ligand then when there is a trans CO ligand. In addition, the overlap is reduced when a CO is trans to N_2 relative to when an N_2 is trans to an N_2 (see Table 9). The overlap decreases when there is a trans CO because the interacting MOs are less localized on the metal as a result of the better capability of CO to back-bond. On the basis of the MO energy levels and overlap, the amount of electron density to be transferred is expected to be less when there is a trans CO. As a consequence the bonding interaction involves more electrons ($\sim$0.07) when N_2 is trans to another N_2, as opposed to when an N_2 is trans to a CO. Then, it is clear that *the lack of a CO trans effect is a strong, if not dominating, factor in the predicted increase in the Cr−N_2 bond energy of $Cr(N_2)_6$*. Calculations indicate that the bond dissociation energy for $Cr(N_2)_6$ should be as large as that for $Cr(CO)_5(N_2)$, although to our knowledge there is no experimental data on the bond dissociation enthalpy for $Cr(N_2)_6$. The increase in stability of $Cr(N_2)_6$ relative to the other dinitrogen complexes is related to the lack of a CO ligand bound to the metal, which manifests itself in the energy decomposition terms, populations and overlaps, which are very similar to those obtained for the $n = 4$ and 5 complexes for an N_2 trans to another N_2.

As a consequence of the trans effect, all of the dinitrogen complexes with N_2 trans to a CO will preferentially lose this N_2. This is consistent with calculations of the relative energies of the resulting unsaturated product. N_2 dissociation from *cis*-$Cr(CO)_2(N_2)_4$ can generate two different $Cr(CO)_2(N_2)_3$ isomers (see below), but the isomer resulting from dissociation of an N_2 trans to CO is 5.5 kcal/mol lower in energy than the isomer resulting from dissociation of an N_2 trans to an N_2. Similar

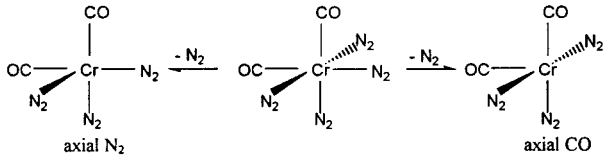

behavior is observed for N_2 dissociation from $Cr(CO)(N_2)_5$. The $Cr(CO)(N_2)_4$ isomer resulting from dissociation of an N_2 trans to a CO is 5.9 kcal/mol lower in energy than that resulting from dissociation of an N_2 trans to another N_2.

Another interesting aspect of the experimental observations of Turner et al.[8] is that when multiple isomers are possible the isomer containing the largest number of N_2 ligands trans to CO is observed to be thermodynamically more stable. The same result is also obtained from calculations. Although at first glance it seems contradictory that *the isomer with the weakest Cr−N_2 bond is the thermodynamically more stable compound*, it must be kept in mind that, although the $Cr-N_2$ bonds are weakened by having a trans CO, the Cr−CO bonds are strengthened *by not* having a trans CO. Calculations indicate that the increase in the Cr−CO bond energies is larger than the decrease in the $Cr-N_2$ bond energies, such that the isomer with more N_2 ligands trans to CO ligands is the lower energy species. This result is also in accord with the better electron accepting ability of CO when compared to N_2. Given that the electron density available for back-bonding is similar in both isomers, it would be less favorable to have two CO ligands trans to each other competing for a portion of the available electron density.

Thus, the $Cr-N_2$ bond strength and stability of the chromium carbonyl dinitrogen complexes are principally determined by the orbital interactions, which, to a large extent, depend on the position of the dissociating N_2 ligand with respect to the CO ligands in the complex.

Now that we have developed some insights into the observed trends in the $Fe-N_2$ and $Cr-N_2$ bond energies as a function of increasing numbers of dinitrogen ligands, it will prove useful to evaluate how much the metal−C and C−O bonds are affected by the consecutive replacement of CO by N_2 ligands.

G. Effect of Dinitrogen Substitution on Metal-C and C−O Bonding. Table 10 contains a summary of the effect of dinitrogen substitution on Cr−CO interactions, in terms of the energy decomposition analysis and the change in Mulliken's electron populations for the relevant chromium complexes. For the dinitrogenated chromium complexes, the total Cr−CO interaction energy ($\Delta E_{oi} + \Delta E_{steric}$) decreases as the number of nitrogen ligands increases. This trend is accompanied by a decrease in the Cr−CO bond energy and a lengthening of the Cr−C bond with increasing *n*. In addition, the substitution of a N_2 for a CO leads to less electron density on the metal fragment (less basic). Therefore, the demand for electron density to back-bond to the CO ligand(s) has to be supplied by the metal itself, consistent with the increasing gross positive charge on the metal. The CO trans effect is again evident in the trends in bond energies. Both orbital and steric interactions are larger for any CO trans to an N_2 compared to a CO that is trans to another

TABLE 10. Energy Decomposition,[a] Gross Mulliken Populations Changes ($P(i)_j$, i = L for Ligand, or fr for Metal Fragment), Bond Lengths, and Force Constants for Cr−CO Interaction in $Cr(CO)_{6-n}(N_2)_n$

	$n=0$	$n=1$	$n=2$	$n=3$	$n=4$	$n=5$
ΔE_{tot}	43.8	49.6 (41.6)	47.7 (39.6)	46.2	45.0	43.5
ΔE_{oi}	78.2	89.9 (77.4)	88.5 (76.4)	87.1	85.3	83.0
ΔE_{steric}	−34.6	−40.6 (−35.8)	−40.8 (−36.8)	−40.9	−40.3	−39.5
ΔE_{pauli}	−114.2	−127.8 (−115.0)	−126.8 (−115.5)	−125.5	−122.6	−119.2
ΔE_{elst}	79.6	87.2 (79.2)	86.0 (78.7)	84.6	82.3	79.7
$-P(L)_\sigma$	0.39	0.41 (0.38)	0.39 (0.36)	0.38	0.36	0.35
$P(L)_{bb}$	0.40	0.44 (0.39)	0.44 (0.39)	0.44	0.43	0.42
$P(fr)_\sigma$	0.34	0.38 (0.35)	0.40 (0.35)	0.40	0.41	0.40
$-P(fr)_{bb}$	0.32	0.34 (0.31)	0.33 (0.30)	0.32	0.32	0.31
$r(C-O)^b$	1.162	1.165 (1.162)	1.165 (1.162)	1.166	1.165	1.165
$r(Cr-C)^b$	1.894	1.861 (1.897)	1.864 (1.900)	1.866	1.868	1.871
$Z(Cr)^c$	0.624	0.699	0.762	0.815	0.862	0.909

[a] Energies in kcal/mol; values in parentheses correspond to CO trans to another CO. [b] Bond lengths (r) in Å. [c] Mulliken charge in the metal.

CO. The trans effect is also reflected in the Cr−C and C−O bond distances. Any CO trans to another CO has longer Cr−C bonds and shorter C−O bonds than those trans to an N_2. However, the C−O bond distance changes little as the number of N_2 ligands increases. The trends mentioned above can be interpreted in terms of the standard models for CO bonding.[12,63] As would be anticipated from such models, the CO stretching frequencies for the most thermodynamically stable isomers in the chromium series decrease as the number of N_2 ligands increase (Figure 6). To follow the shift of the CO stretching frequencies as a function of the number of N_2 ligands, the CO stretching modes in the lower symmetry molecules that correlate with the t_{1u} (IR active) and a_{1g} (IR inactive) modes[64] of $Cr(CO)_6$ were calculated. It is often assumed[63] that a trend of *decreasing* CO stretching frequency is associated with a *decrease* in the metal−carbon bond length. Such arguments are based on the assumption that a shortening of the metal−carbon bond occurring in concert with a lengthening of the C−O bond can be viewed as a manifestation of the factor(s) that leads to a decrease in the CO vibrational frequency. For example, the t_{1u} CO stretch in $Cr(CO)_6$ is at 1987 cm^{-1} and the Cr−C bond length is 1.894 Å, whereas the symmetry correlated e mode in $Cr(CO)_5(N_2)$ is at 1975 cm^{-1} and the Cr−C bond length is 1.861 Å. In this comparison, the *decreasing* CO stretching frequency is accompanied by a *decrease* in the Cr−C bond distance, as anticipated, because the coordinatively unsaturated species is the same in both cases: $Cr(CO)_5$. Although this picture may hold when considering the effect of substitution of one ligand for another around an otherwise unchanged metal center, *it is not necessary valid* when considering the effect of addition of a ligand to different coordinatively unsaturated complexes, as is the case for the series of dinitrogenated complexes. In this latter case, caution has to be exercised in attempting to use CO vibrational frequencies to determine changes in the metal−carbon bond order. For example, in the $Cr(CO)_{6-n}(N_2)_n$ series, the Cr−C bond length *increases* as n increases, although the corresponding CO frequencies are *decreasing* (see Table 10). Although there are variations in the magnitude of the force constants as n increases, with the exception of the $Cr(CO)_3(N_2)_3$ complex, the trend in the Cr−C force constants is matched by a corresponding trend in the Cr−C bond length: an increase in bond length is mirrored by a decrease in the force constant and visa versa.

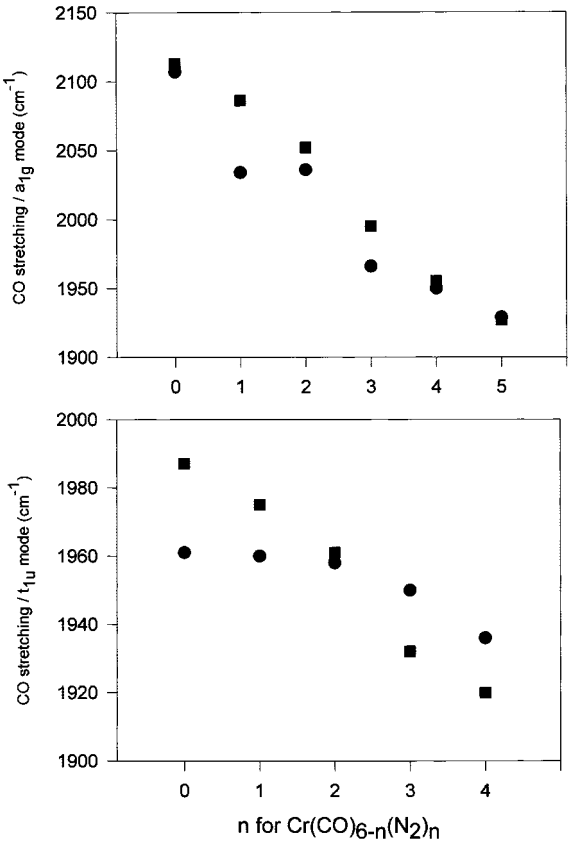

Figure 6. Calculated (●) and experimental (■) C−O stretching frequencies for the complexes $Cr(CO)_{6-n}(N_2)_n$. Top and bottom correspond to modes correlated to the a_{1g} and t_{1u} modes of $Cr(CO)_6$, respectively.

In addition, the trans effect is manifested in the magnitude of the calculated force constants. Figure 7 shows the variation in Cr−C and C−O force constant with bond length for $Cr(CO)_5(N_2)$ and $Cr(CO)_4(N_2)_2$. These two complexes have two

TABLE 11: Energy Decomposition[a] and Gross Mulliken Populations Changes ($P(i)_j$, i = L for Ligand, or fr for Metal Fragment) for Fe−CO Interaction in $Fe(CO)_{5-n}(N_2)_n$

	$n=0$	$n=1$	$n=2$	$n=3$	$n=4$
ΔE_{tot}	48.7	50.2	47.4	52.4	49.4
	(52.4)	(49.8)	(56.0)	(53.2)	
ΔE_{oi}	93.2	99.8	94.3	110.3	102.5
	(95.1)	(90.5)	(101.6)	(101.8)	
ΔE_{steric}	−44.5	−49.6	−46.9	−57.9	−53.4
	(−42.7)	(−41.4)	(−45.7)	(−48.6)	
ΔE_{pauli}	−155.6	−167.8	−159.2	−185.2	−174.3
	(−141.1)	(−136.3)	(−146.1)	(−149.7)	
ΔE_{elst}	111.1	118.2	112.3	127.3	120.9
	(98.4)	(94.9)	(100.4)	(101.1)	
$-P(L)_\sigma$	0.44	0.44	0.42	0.44	0.42
	(0.46)	(0.44)	(0.45)	(0.44)	
$P(L)_{bb}$	0.44	0.45	0.45	0.50	0.48
	(0.44)	(0.42)	(0.45)	(0.45)	
$P(fr)_s$	0.41	0.43	0.46	0.56	0.49
	(0.40)	(0.38)	(0.41)	(0.42)	
$-P(fr)_{bb}$	0.49	0.54	0.49	0.58	0.53
	(0.44)	(0.43)	(0.46)	(0.45)	
$r(C-O)^b$	1.163	1.165	1.165	1.168	1.168
	(1.160)	(1.160)	(1.163)	(1.163)	
$r(Fe-C)^b$	1.792	1.779	1.787	1.764	1.775
	(1.794)	(1.801)	(1.768)	(1.773)	
$Z(Fe)^c$	0.422	0.467	0.511	0.617	0.654

[a] Energies in kcal/mol; values in parentheses corresponds to CO in the axial position. [b] Bond lengths in Å. [c] Mulliken charge on the metal.

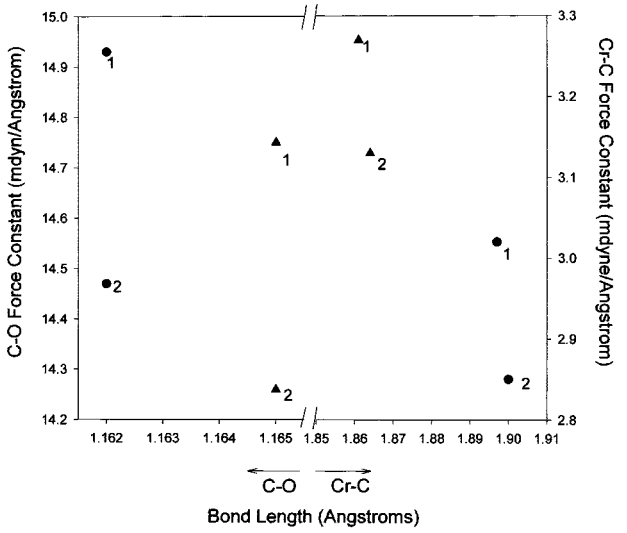

Figure 7. Calculated C−O and Cr−C force constants for (1) $Cr(CO)_5(N_2)$ and (2) $Cr(CO)_4(N_2)_2$. Circles are data for CO trans to CO and triangles for CO trans to N_2.

different types of CO ligands: some are trans to another CO and some are trans to a N_2 ligand. As seen in Figure 7, the Cr−C force constant for these complexes is larger for a CO trans to N_2 than for a CO trans to CO, consistent with shorter calculated Cr−C bond lengths for COs trans to N_2.

For the $Fe(CO)_{5-n}(N_2)_n$ complexes, the trends in metal−CO interaction energies are dependent on whether the CO is in the axial or the equatorial position. Table 11 contains data for the lowest energy complexes in the series. When an axial CO is replaced by an N_2 the total interaction energy increases for the equatorial CO(s) and decreases for any remaining axial COs. The trend in the interaction energy is similar to that found for the Fe−N_2 interactions discussed in section III.B., and it is reflected in the Fe−C bond length. However, comparisons with trends in the CO stretching frequencies cannot be made for the entire series of iron complexes because a complete set of experimental frequencies is not available. Nevertheless, as n increases, calculations predict an increase in frequency for the a_1' symmetry correlated mode and a trend of decreasing frequency for the a_2'' and e' modes. The trend for the calculated a_1' vibrational mode is opposite to what is seen for the series of chromium complexes and deserves further consideration.

IV. Conclusions

Geometries were optimized and bond energies and frequencies were calculated for $Fe(CO)_{5-n}(N_2)_n$, $n = 0-5$, and $Cr(CO)_{6-n}(N_2)_n$, $n = 0-6$, complexes using DFT with the BP86 functional. The M−CO bond enthalpies in $Fe(CO)_5$ and $Cr(CO)_6$ were calculated to be 43.4 and 41.2 kcal/mol, respectively, in good agreement with the experimental values of 41 ± 2[36] for $Fe(CO)_5$ and 37 ± 2[36] and 37 ± 5[37] for $Cr(CO)_6$. For metal−N_2 bond enthalpies, the calculated value for the Cr−N_2 bond dissociation enthalpy in $Cr(CO)_5(N_2)$ of 21.1 kcal/mol agrees well with the experimental value[52] in heptane solution of 19 ± 1. Although there are no quantitative experimental data for the bond enthalpies for the other chromium complexes, the bond enthalpy calculations for *cis*-$Cr(CO)_4(N_2)_2$ and *fac*-$Cr(CO)_3(N_2)_3$ agree well with estimates of the bond enthalpies that can be obtained from the half-lives for these complexes which have been reported in low-temperature condensed phase experiments. The calculated value for the Fe−N_2 bond enthalpy for eq-$Fe(CO)_4(N_2)$ (19.0 kcal/mol) is in agreement with the gas-phase experimental value[10] (17.6 ± 1.8 kcal/mol). The experimental Fe−N_2 bond enthalpy in the $Fe(CO)_3(N_2)_2$ complex was determined[10] to be 9.0 ± 4.6 kcal/mol. Calculations indicate that the cis-(a,e) isomer is the most stable, which is consistent with the pattern and positions of the calculated and experimental CO stretching frequencies. The calculated bond enthalpy for this isomer is 13.6 kcal/mol. Bond enthalpies of 11.4 and 8.1 kcal/mol were calculated for the cis-(e,e) and trans isomers, respectively. Comparisons of calculated frequencies for singlet and triplet $Fe(CO)_3(N_2)$ with experimental data are consistent with $Fe(CO)_3(N_2)$ having a triplet ground state with the N_2 in the pseudoaxial position.

In general, calculated metal−CO bond energies are almost twice as large as the corresponding metal−N_2 bonds because CO is better at both donating and accepting electron density

than N_2. In both series of complexes, the metal−N_2 bond energy decreases as the number of N_2 ligands is increased, with the exception of the $Cr(N_2)_6$. The predicted increase in the Cr−N_2 bond energy of $Cr(N_2)_6$ relative to the other complexes in the chromium series is due to the lack of CO a "trans effect" which is present in the other dinitrogen substituted compounds in this series. This type of trans effect lowers the bond dissociation energy of the N_2 ligand trans to the CO. Additionally, a CO trans to an N_2 ligand weakens that bond as a result of the stronger back-bonding ability of CO with respect to N_2. Thus, when a chromium complex has dinitrogen ligands trans to both CO and N_2, the dinitrogen trans to CO dissociates preferentially. The trans effect is also manifested in the relative stability of isomeric chromium complexes. Both experiments and calculations indicate that the lowest energy isomer is the one with a larger number of N_2 ligands trans to CO ligands. This is because, although having a trans CO weakens the Cr−N_2 bonds, the Cr−C bonds are strengthened by not having a trans CO. The trans effect is also evident in the chromium complexes, where an N_2 ligand trans to a CO ligand leads to a stronger Cr−C bond at the expense of the C−O bond. In these complexes the C−O stretching frequencies decrease as the number of N_2 ligands increase. This is a result of a reduction in the competition for the electron density that is available for back-bonding to the CO.

For iron complexes where there can be axial and equatorial dinitrogen ligands, there is a preference for dissociation of the equatorial over the axial N_2 ligand because the deformation energy is smaller for an equatorial ligand loss. More importantly, the decrease in bond energy with increasing numbers of N_2 ligands is not the result of a decrease in the net interaction energy of the complex. Rather, it is dominated by the amount of energy required to deform the reacting moieties into geometries that correspond to their configuration in the equilibrium geometries of the resulting complex. On the other hand, the deformation energy in the chromium complexes is minimal, and the Cr−N_2 bond energy is effectively determined by the orbital interaction energy. Although the orbital interactions of iron with dinitrogen are larger than those of chromium with dinitrogen, the much larger deformation energy for the iron complexes accounts for the differences in stability of carbonyl dinitrogen iron complexes relative to the analogous chromium complexes. Thus, we have demonstrated that the magnitude of the deformation energy can be the dominant factor in determining the change in bond dissociation energy among the iron dinitrogen complexes and between a given iron dinitrogen complex and its chromium analogue. However, interestingly, this factor is generally not in the description of factors that determine bond dissociation energies in organometallic compounds that appears in standard textbooks.

Acknowledgment. We acknowledge support of this work by the National Science Foundation under Grant #97-34891. We appreciate the help of Dale Braden and Tom Pollard at Schrodinger Inc. who provided the software to obtain the force constants.

Supporting Information Available: Additional tables showing the calculated geometrical parameters for all of the 18- and 16-electron complexes mentioned in this manuscript are available free of charge via the Internet at http//pubs.acs.org.

References and Notes

(1) Marks, T. J. In *Bonding Energetics in Organometallic Compounds*; ACS Symposium Series 428; American Chemical Society: Washington DC, 1990; Chapter 1.

(2) Laird, B. B.; Ross, R. B.; Ziegler, T. In *Chemical Applications of Density Functional Theory*; ACS Symposium Series 629; American Chemical Society: Washington DC, 1996; Chapter 2.

(3) *Density Functional Methods in Chemistry*, Labanowski, J. K., Andzelm, J. W., Eds.; Springer-Verlag: New York, 1991.

(4) (a) Ziegler, T. *Chem. Rev.* **1991**, *91*, 651. (b) Ziegler, T. *Can. J. Chem.* **1995**, *73*, 743.

(5) (a) Ziegler, T.; Rauk, A. *Theor. Chim. Acta* **1977**, *46*, 1. (b) Ziegler, T.; Rauk, A. *Inorg. Chem.* **1979**, *18*, 1558. (c) Ziegler, T.; Rauk, A. *Inorg. Chem.* **1979**, *18*, 1755.

(6) Bickelhaupt, F. M.; Nibbering, N. M.; van Wezenbeek, E. M.; Baerends, E. J. *J. Phys. Chem.* **1992**, *96*, 4864.

(7) (a) Morokuma, K. *Acc. Chem. Res.* **1977**, *10*, 294. (b) Kitaura, K.; Morokuma, K. *Int. J. Quantum Chem.* **1976**, *10*, 325.

(8) Turner, J. J.; Simpson, M. B.; Poliakoff, M.; Maier, W. B., II; Graham, M. A. *Inorg. Chem.* **1983**, *22*, 911.

(9) DeVore, T. C. *Inorg. Chem.* **1976**, *15*, 1315.

(10) Wang, J.; Long, G. T.; Weitz, E. *J. Phys. Chem. A* **2001**, *105*, 3765.

(11) Doeff, M. M.; Parker, S. F.; Barrett, P. H.; Pearson, R. G. *Inorg. Chem.* **1984**, *23*, 4108.

(12) Crabtree, R. H. *The Organometallic Chemistry of the Transition Metals*, 2nd ed.; Wiley and Sons: New York, 1994.

(13) *Jaguar 3.5* and *4.0*; Schrodinger, Inc.: Portland, OR, 1998−1999.

(14) (a) Friesner, R. A. *Chem. Phys. Lett.* **1985**, *116*, 39. (b) Friesner, R. A. *J. Chem. Phys.* **1987**, *86*, 3522. (c) Friesner, R. A. *J. Phys. Chem.* **1988**, *92*, 3091. (d) Langlois, J. M.; Muller, R. P.; Coley, T. R.; Goddard, W. A., III; Ringnalda, M. N.; Won, Y.; Friesner, R. A. *J. Chem. Phys.* **1990**, *92*, 7488. (e) Ringnalda, M. N.; Belhadj, M.; Friesner, R. A. *J. Chem. Phys.* **1990**, *93*, 3397. (f) Friesner, R. A. *Annu. Rev. Phys. Chem.* **1991**, *94*, 8152.

(15) Slater, J. C. *Quantum Theory of Molecules and Solids, Vol. 4: The Self-Consistent Field for Molecules and Solids*; McGraw-Hill: New York, 1974.

(16) Vosko, S. H.; Wilk, L.; Nusair, M. *Can. J. Phys.* **1980**, *58*, 1200.

(17) Becke, A. D. *Phys. Rev. A* **1988**, *38*, 309818.

(18) (a) Perdew, J. P. *Phys. Rev. B* **1986**, *33*, 8822. (b) Perdew, J. P. *Phys. Rev. B* **1986**, *34*, 7406.

(19) Hay, P. J.; Wadt, W. R. *J. Chem. Phys.* **1985**, *82*, 299.

(20) *Jaguar 3.5*; User's Guide, Schrodinger, Inc.: Portland, OR, 1998; p 284.

(21) (a) Ditchfield, R.; Hehre, W. J.; Pople, J. A. *J. Chem. Phys.* **1971**, *54*, 724. (b) Hehre, W. J.; Pople, J. A. *J. Chem. Phys.* **1972**, *56*, 4233. (c) Binkley, J. S.; Pople, J. A. *J. Chem. Phys.* **1977**, *66*, 879. (d) Hariharan, P. C.; Pople, J. A. *Theor. Chim. Acta* **1973**, *28*, 213. (e) Hehre, W. J.; Ditchfield, R.; Pople, J. A. *J. Chem. Phys.* **1972**, *56*, 2257 (f) Francl, M. M.; Pietro, W. J.; Hehre, W. J.; Binkley, J. S.; Gordon, M. S.; DeFrees, D. J.; Pople, J. A. *J. Chem. Phys.* **1982**, *77*, 3654.

(22) (a) Clark, T.; Chandrasekhar, J.; Spitznagel, G. W.; Schleyer, P. von R. *J. Comput. Chem.* **1983**, *4*, 294. (b) Frisch, M. J.; Pople, J. A.; Binkley, J. S. *J. Chem. Phys.* **1984**, *80*, 3265. (c) Krishnan, R.; Binkley, J. S.; Seeger, R.; Pople, J. A. *J. Chem. Phys.* **1980**, *72*, 650. (d) McLean, A. D.; Chandler, G. S. *J. Chem. Phys.* **1980**, *72*, 5639.

(23) Bérces, A.; Ziegler, T. *J. Phys. Chem.* **1995**, *99*, 11417.

(24) (a) Bérces, A.; Ziegler, T. *Topics in Current Chemistry*; Nalewajski, R. F., Ed.; Springer-Verlag: New York, 1996; Vol. 182, p 42. (b) Bérces, A.; Ziegler, T. *J. Phys. Chem.* **1994**, *98*, 13233.

(25) Deakyne, C. A.; Liebman, J. F. In *Encyclopedia of Computational Chemistry*; Schleyer, P. v. R., Allinger, N. R., Clark, T., Gasteiger, J., Kollman, P. A., Schaefer, H. F., III, Schreiner, P. R., Eds.; Wiley: Chichester, U.K., 1998; Vol. 2, p 1439.

(26) Boys, S. F.; Bernardi, F. *Mol. Phys.* **1970**, *19*, 553.

(27) (a) *Amsterdam Density Functional*, ADF; SCM, Vrije Universiteit: The Netherlands, 1999. (b) Baerends, E. J.; Ellis, D. E.; Ros, P. *Chem. Phys.* **1973**, *2*, 41. (c) Versluis, L.; Ziegler, T. *J. Chem. Phys.* **1988**, *88*, 322. (d) te Velde, G.; Baerends, E. J. *J. Comput. Chem.* **1992**, *99*, 84. (e) Fonseca Guerra, C.; Snijders, J. G.; te Velde, G.; Baerends, E. J. *Theor. Chem. Acc.* **1998**, *99*, 391.

(28) (a) Snijders, G. J.; Baerends, E. J.; Vernooijs, P. *At. Data Nucl. Data Tables* **1982**, *26*, 483. (b)Vernooijs, P.; Snijders, G. J.; Baerends, E. J. *Slater Type Basis Functions for the whole Periodic System*, internal report; Free University of Amsterdam: Amsterdam, The Netherlands, 1981.

(29) Krijn, J.; Baerends, E. J. *Fit functions in the HFS-method*, internal report; Free University of Amsterdam: Amsterdam, The Netherlands, 1984.

(30) Mulliken, R. S. *J. Chem. Phys.* **1955**, *48*, 1833.

(31) Beagley, B.; Schmidling, D. *J. Mol. Struct.* **1974**, *22*, 466.

(32) Braga, D.; Grepione, F.; Orpen, A. G. *Organometallics* **1993**, *12*, 1481.

(33) Jost, A.; Rees, B.; Yelon, W. B. *Acta Crystallogr.* **1975**, *B31*, 264934.

(34) van Wüllen, C. *J. Chem. Phys.* **1996**, *105*, 5485.

(35) Wang, W.; Weitz, E. *J. Phys. Chem.* **1997**, *101*, 2358

(36) Rosa, A.; Ehlers, A. W.; Baerends, E. J.; Snijders, J. G.; te Velde, G. *J. Phys. Chem.* **1996**, *100*, 5690.
(37) Herzberg, G. *Molecular Spectra and Molecular Structure I. Spectra of Diatomic Molecules*; Krieger Publishing Co.: Malabar, FL, 1989.
(38) Lewis, K. E.; Golden, D. M.; Smith, G. P. *J. Am. Chem. Soc.* **1984**, *106*, 3905.
(39) Bernstein, M.; Simon, J. D.; Peters, K. S. *Chem. Phys. Lett.* **1983**, *100*, 241.
(40) Li, J.; Schreckenbach, G.; Ziegler, T. *J. Am. Chem. Soc.* **1995**, *117*, 486.
(41) Radius, U.; Bickelhaupt, F. M.; Ehlers, A. W.; Goldberg, N.; Hoffmann, R. *Inorg. Chem.* **1998**, *37*, 1080.
(42) Delley, B.; Wrinn, M.; Luthi, H. P. *J. Chem. Phys.* **1994**, *100*, 5785.
(43) Ehlers, A. W.; Frenking, G. *Organometallics* **1995**, *14*, 423.
(44) Ehlers, A. W.; Frenking, G. *J. Am. Chem. Soc.* **1994**, *116*, 1514.
(45) Poliakoff, M.; Weitz, E. *Acc. Chem. Res.* **1987**, *20*, 408.
(46) Graham, M. A.; Poliakoff, M.; Turner, J. J. *J. Chem. Soc. A* **1971**, 2939.
(47) Yamamoto, A. *Organotransition Metal Chemistry, Fundamental Concepts and Applications*; Wiley: New York, 1986.
(48) Ricca, A.; Bauschlicher, C. W., Jr. *J. Phys. Chem.* **1994**, *98*, 12899.
(49) (a) Poliakoff, M.; Turner, J. J. *J. Chem. Soc., Dalton Trans.* **1974**, 2276. (b) Cooper, A. I.; Poliakoff, M. *Chem. Phys. Lett.* **1993**, *212*, 611.
(50) House, P. G.; Weitz, E. *Chem. Phys. Lett.* **1997**, *266*, 239.
(51) Dapprich, S.; Pidun, U.; Ehlers, A. W.; Frenking, G. *Chem. Phys. Lett.* **1995**, *242*, 521.
(52) Walsh, E. F.; Popov, V. K.; George, M. W.; Poliakoff, M. *J. Phys. Chem.* **1995**, *99*, 12016.
(53) As an approximate value, the experimental preexponetial for dissociation of H_2 from $Cr(CO)_5(H_2)$ has been used from Wells, J. R.; House, P. G.; Weitz, E. *J. Phys. Chem.* **1994**, *98*, 8343.
(54) (a) Margl, P.; Deng, L. Q.; Ziegler, T. *J. Am. Chem. Soc.* **1998**, *120*, 5517. (b) Michalak, A.; Ziegler, T. *J. Am. Chem. Soc.* **2000**, *122*, 1850.
(55) Martinho Simões, J. A.; Beauchamp, J. L. *Chem. Rev.* **1990**, *90*, 629.
(56) (a) Wang, W.; Weitz, E. Unpublished results on DFT calculation of bond energies for $M(CO)_4(C_2X_4)$ (M = Fe and Cr; X = H, F, and Cl). (b) Cedeño, D. L.; Weitz, E. Unpublished results on DFT calculations for $Fe(CO)_4(C_2X_4)$ (X = H, F, Cl, Br, I, and CN).
(57) Sanderson, R. T. Chemical Bonds and Bond Energy. In *Physical Chemistry*; Loebl, E. M., Ed.; Academic Press: New York, 1976; Vol. 21.
(58) (a) Williams, R. J. P. *Eur. J. Biochem.* **1995**, *234*, 363. (b) Armstrong, F. A.; Williams, R. J. P. *FEBS Lett.* **1999**, *451*, 91.
(59) (a) Britt, B. M. *Biophys. Chem.* **1997**, *69*, 63. (b) Britt, B. M. *J. Theor. Biol.* **1993**, *164*, 181.
(60) Bérces, A. *Inorg. Chem.* **1997**, *36*, 4831.
(61) (a) Warshel, A. *Theor. Chem. Acc.* **2000**, *103*, 337. (b) Warshel A. *Proc. Natl. Acad. Sci. U.S.A.* **1976**, *75*, 5250. (c) Warshel A.; Florián, J. *Proc. Natl. Acad. Sci. U.S.A.* **1998**, *95*, 5950.
(62) Olson, M. H. M.; Ryde, U.; Roos, B. *J. Inorg. Biochem.* **1999**, *74*, 254.
(63) Cotton, F. A.; Wilkinson, G.; Murillo, C. A.; Bochmann, M. *Advanced Inorganic Chemistry*, 6th ed.; Wiley and Sons: New York, 1999.
(64) Braterman, P. S. *Organometallic Chemistry Series: Metal Carbonyl Spectra*; Maitlis, P. M., Stone, F. G. A., West, R., Eds.; Academic Press: London, 1975.